medRxiv preprint doi: https://doi.org/10.1101/2024.03.18.24304520; this version posted March 19, 2024. The copyright holder for this preprint (which was not certified by peer review) is the author/funder, who has granted medRxiv a license to display the preprint in perpetuity. It is made available under a CC-BY-NC-ND 4.0 International license .

Title: A Dynamic Time-Series Model of Oxygen Consumption during Paediatric Cardiopulmonary Bypass.

Short Title: Dynamic VO_2i Prediction During Paediatric CPB

Authors: Mansour T. A. Sharabiani, PhD[1†], Richard W. Issitt, DClinP[2,3,4†], Alireza S. Mahani, PhD[5†], Yadav Srinivasan, MD[6], Serban Stoica, FRCS MD[7].

Affiliations:

[1] School of Public Health, Imperial College, London, United Kingdom

[2] Centre for Heart Failure, Transplantation and Extracorporeal Support, UCL Institute for Cardiovascular Science, UCL, London, United Kingdom

[3] Perfusion Department, Great Ormond Street Hospital for Children, London, United Kingdom

[4] Data Research, Innovation and Virtual Environments Unit, Great Ormond Street Hospital for Children, London, United Kingdom

[5] Davidson Kempner Capital Management, New York, United States of America

[6] Cardiac Surgery Department, Great Ormond Street Hospital for Children, London, United Kingdom

[7] Cardiac Surgery Department, Bristol Royal Children's Hospital, Bristol, United Kingdom

[†] These authors contributed equally to this work.

Corresponding Author:

Dr Richard Issitt

Centre for Heart Failure, Transplantation and Extracorporeal Support, Research Department of Children's Cardiovascular Disease, UCL Institute of Cardiovascular Science, London, United Kingdom.

Email: richard.issitt@ucl.ac.uk. Tel: +44 (0) 20 7813 8287.

NOTE: This preprint reports new research that has not been certified by peer review and should not be used to guide clinical practice.

medRxiv preprint doi: https://doi.org/10.1101/2024.03.18.24304520; this version posted March 19, 2024. The copyright holder for this preprint (which was not certified by peer review) is the author/funder, who has granted medRxiv a license to display the preprint in perpetuity. It is made available under a CC-BY-NC-ND 4.0 International license .

Abstract

Background: During cardiopulmonary bypass (CPB), maintaining adequate oxygen consumption (VO_2i) can only be achieved indirectly either by modifying oxygen delivery (DO_2i) through its component parts or by modulating metabolic demand through altering body temperature. The body reacts to these actions by changing OER and consequently VO_2i. Understanding the body's adaptive OER dynamics can elucidate its oxygen consumption goals during CPB and help improve our ability to safely manage the patient's journey.

Methods: An autoregressive, integrated time-series model was trained on granular perfusion data from 879 paediatric patients (age: newborn to 18 years old) undergoing 963 CPB operations, with the outcome variable being the minute-by-minute changes in the logit transformation of OER. Variables were cardiac index, haemoglobin concentration, oxygen saturation of arterial haemoglobin and temperature. An explicit 'disequilibrium term group' was also included, proportional to the difference between the logarithm of VO_2i and logarithm of a 'latent' (i.e. unobserved) oxygen demand - or 'target' VO_2 (tVO_2i) - term, with the logarithm of tVO_2i assumed to be a linear function of body temperature (the Van't Hoff model). The trained time-series models were studied using permutation-based variable importance, deterministic and stochastic simulations, and subgroup analysis by acute kidney injury (AKI) grade and by temperature.

Results: Model coefficients are consistent with an adaptive OER response to keep VO_2i in line with tVO_2i, according to body temperature. This adaptation consists of a primary rapid response for 5-10 minutes, and a secondary slow response that is estimated to last up to several hours. The model reproduces the hyperbolic shape of DO_2i-VO_2i curves - first published in 1982 - as an artefact of insufficient wait times between equilibrium-state transitions. Asymptotically, however, the model converges to a piecewise linear relationship between DO_2i and VO_2i, with supply-independence of oxygen consumption occurring above a threshold DO_2i. Subgroup analysis by temperature suggests that the dependence of tVO_2i on temperature (expressed as Q10) may be significantly stronger at low temperatures (< 28C) than at high temperatures (> 28C).

medRxiv preprint doi: https://doi.org/10.1101/2024.03.18.24304520; this version posted March 19, 2024. The copyright holder for this preprint (which was not certified by peer review) is the author/funder, who has granted medRxiv a license to display the preprint in perpetuity. It is made available under a CC-BY-NC-ND 4.0 International license .

Conclusions: This study proposes a physiologically plausible model of OER changes during CPB that is consistent with past experimental data. While during CPB, under-oxygenation is the dominant risk in the long term, slow adaptation of OER during CPB creates short-term opportunities for over-oxygenation following significant changes in variables such as cardiac index. The model provides well-defined values for tVO_2i at a given temperature, paving the way for further research into the effects of over- and under-oxygenation during CPB on postoperative outcomes such as AKI, and hence improvements in goal-directed perfusion protocols.

medRxiv preprint doi: https://doi.org/10.1101/2024.03.18.24304520; this version posted March 19, 2024. The copyright holder for this preprint (which was not certified by peer review) is the author/funder, who has granted medRxiv a license to display the preprint in perpetuity. It is made available under a CC-BY-NC-ND 4.0 International license .

Nonstandard Abbreviations and Acronyms

- AKI: acute kidney injury
- GARIX: global autoregressive Integrated (time-series model) with exogenous variables
- GARIX+: GARIX model, plus a disequilibrium term group (in addition to autoregressive and exogenous term groups)
- ATG: autoregressive term group
- BSA: body surface area (m^2)
- CI: cardiac index (blood flow indexed BSA) ($L/min/m^2$)
- CPB: cardiopulmonary bypass
- CV: cross-validation
- DHCA: deep hypothermic circulatory arrest
- DO_2: oxygen delivery (mL/min)
- DO_2i: oxygen delivery, indexed to BSA ($mL/min/m^2$)
- DTG: disequilibrium term group
- EHR: electronic health record
- ETG: exogenous term group
- GDP: goal-directed perfusion
- Hb: haemoglobin content of blood (g/dL)
- HLM: heart-lung machine
- i.i.d.: Independent and identically distributed
- ML: machine learning
- OER: oxygen extraction ratio
- OG: oxygenation gGap
- OOS: out-of-sample
- PaO_2: partial pressure of oxygen (kPa)
- PVI: permutation-based variable importance
- Q10: multiplicative increase in the resting metabolic rate for every 10℃ increase in body temperature
- RBCs: red blood cells
- RMR: resting metabolic rate

medRxiv preprint doi: https://doi.org/10.1101/2024.03.18.24304520; this version posted March 19, 2024. The copyright holder for this preprint (which was not certified by peer review) is the author/funder, who has granted medRxiv a license to display the preprint in perpetuity. It is made available under a CC-BY-NC-ND 4.0 International license .

- RTO: return-to-equilibrium (an estimated parameter in the GARIX+ model)
- SaO_2: oxygen saturation of arterial blood (scale: 0-100)
- SvO_2: Oxygen saturation of mixed venous blood (scale: 0-100)
- TG: term group
- tVO_2i: target (indexed) oxygen consumption, aka (indexed) oxygen demand (mL/min/m^2)
- tDO_2i: threshold (indexed) oxygen delivery (mL/min/m^2)
- VI: variable importance
- VO_2: oxygen consumption (mL/min)
- VO_2i: oxygen consumption, indexed to BSA (mL/min/m^2)

Clinical Perspective

What Is New?

- This study is the first to present a data-driven, analytical framework for predicting OER changes in response to clinical interventions during CPB.
- Changes in the components of oxygen delivery cause an adaptive OER response to keep oxygen consumption in line with oxygen demand, according to body temperature.
- The dependence of oxygen demand on temperature decreases as temperature increases towards normothermia, inconsistent with the accepted Van’t Hoff equation.
- Children developing AKI exhibit a dampened response to changes in haemoglobin during CPB, with this dampening of response intensifying with AKI severity.

What Are the Clinical Implications?

- This proposed, dynamic model of OER provides a novel framework for goal-directed perfusion by identifying periods of over- and under-oxygenation.

medRxiv preprint doi: https://doi.org/10.1101/2024.03.18.24304520; this version posted March 19, 2024. The copyright holder for this preprint (which was not certified by peer review) is the author/funder, who has granted medRxiv a license to display the preprint in perpetuity. It is made available under a CC-BY-NC-ND 4.0 International license .

- The observed, dampened response to haemoglobin changes in patients that develop AKI can be the foundation of an intraoperative tool for early diagnosis of at-risk patients.

Introduction

During cardiopulmonary bypass (CPB), the heart-lung machine (HLM) takes over the twin functions of perfusion: oxygenation and carbon dioxide removal, and circulation of the blood. Given the central role of perfusion during surgery, much attention has been given to reducing postoperative end-organ dysfunctions via improvements in perfusion strategies, which has led to the advent of the term goal-directed perfusion (GDP). An important prerequisite for GDP is identifying an appropriate, and specific, set of 'goals' for perfusion. Much research has focused on the determination of a threshold for oxygen delivery - indexed to body surface area (BSA) - (DO_2i) for aerobic metabolism, below which the risk of acute kidney injury (AKI) increases (Ranucci *et al*, 2018; Hendrix *et al*, 2019; Dreher *et al*, 2023; Do-Nguyen *et al*, 2023; Hayward *et al*, 2023). Focusing on under-oxygenation risk is motivated by the concept of 'supply-independence of oxygen consumption', which posits that, as long as sufficient oxygen is delivered to the body, it is otherwise capable of extracting what it needs, without the risk of over-oxygenation. This concept is reflected in the piecewise linear (or elbow) model of oxygen consumption vs. oxygen delivery (Figure 1). We refer to the supply-independent oxygen consumption as oxygen demand, or target VO_2i (tVO_2i).

Focusing on a single threshold-DO_2i (tDO_2i) during an entire CPB session, while easy to communicate and implement by practitioners, has a few shortcomings. First, it does not take into account the temperature-dependence of oxygen demand. During CPB, especially one involving Deep Hypothermic Circulatory Arrest (DHCA), the patient's body temperature can change by 20℃ or more. Assuming a Q10 of 2.5, a 20-degree temperature change translates into a more than six-fold variation in oxygen demand during CPB. Using a single tDO_2i for this entire range would be either impractical (satisfying a high tDO_2i would clash with need to reduce flow at times for better visibility during surgery) or unsafe (allowing for a low tDO_2i would endanger the patient during normal temperatures), or both. Secondly, empirical evidence does not support a simple elbow model with a clear-cut tDO_2i. For instance, Fox *et al*, (1982) show that a

medRxiv preprint doi: https://doi.org/10.1101/2024.03.18.24304520; this version posted March 19, 2024. The copyright holder for this preprint (which was not certified by peer review) is the author/funder, who has granted medRxiv a license to display the preprint in perpetuity. It is made available under a CC-BY-NC-ND 4.0 International license .

hyperbolic model (Figure 1) - which is a smooth version of the elbow model - better fits the data from human and animal experiments (Paneth et al, 1957; Cheng et al, 1959; Starr, 1959)[1]. Besides the hyperbolic function, other smooth, saturating functions such as the exponential curve have also been proposed (Lubarsky et al, 1995). Despite better fit, such smooth functions do not provide a well-defined tDO_2i. Ad-hoc substitutes, such as finding the intersection of the 70% confidence bands with the tVO_2i line (Kirklin and Blackstone, 2012), are somewhat arbitrary. One potential advantage of these experiments supporting the textbook model is that the experimental setup presumably allowed for the system to reach steady state before each measurement. However, this advantage is also the reason why such experiments are unlikely to be replicated, especially in humans. On the other hand, technological advances have allowed us to collect temporally granular perfusion data during routine CPB. In these observational settings, variables such as blood flow, haemoglobin concentration, arterial oxygen partial pressure and body temperature are all subject to constant fluctuations, driven by surgical requirements. In other words, we can never assume the system is in a steady state or equilibrium. Yet, after mathematically accounting for system dynamics, one could extract important insights from such granular data about the body and its oxygen uptake mechanisms during CPB, including the dependence of oxygen consumption on oxygen delivery, as well as the dependence of oxygen demand on body temperature. The primary aim of this study is to understand the innate adjustments to OER that occur during CPB to maintain oxygen consumption in line with oxygen demand, as dictated by the resting metabolic rate (RMR). In particular, we create a time-series model to predict the minute-by-minute changes in oxygen extraction rate (OER), as a function of the past and intended (i.e. future) changes in blood flow rate, haemoglobin level, and temperature (exogenous variables), past changes in OER (endogenous variable), and present state of the system. The secondary aim of the study was to understand how coefficients and model performance changed in patients that developed AKI compared to those that did not. Finally, we aimed to examine the relationship between oxygen demand and temperature to determine if it follows the simple parametric form of Van't

[1] Note that the hyperbolic function is mathematically equivalent to the Michaelis-Menten formulation, a terminology used for describing enzymatic reactions.

medRxiv preprint doi: https://doi.org/10.1101/2024.03.18.24304520; this version posted March 19, 2024. The copyright holder for this preprint (which was not certified by peer review) is the author/funder, who has granted medRxiv a license to display the preprint in perpetuity. It is made available under a CC-BY-NC-ND 4.0 International license .

Hoff, which has been the prevailing model in the literature. This was undertaken by conducting a subgroup analysis of the data by temperature band over the entire range of temperatures recorded in our granular CPB data.

Methods

Study Design and Participants

This was a retrospective analysis of patients aged younger than 18 years (maximum age treated at the institution), who underwent cardiac surgery with CPB at Great Ormond Street Hospital for Children, London. The cohort was selected using a National Institute for Cardiovascular Outcomes Research (NICOR) validated data set for patients operated on between April 2019 and April 2021. All clinical data from 879 paediatric patients undergoing 963 CPB operations were collated in a research platform within the hospital's governance structure and de-identified before analysis. Institutional approval was given for the undertaking of this project (audit number 3045). Individual consent was not required because only routinely collected de-identified hospital data were evaluated within the secure digital research environment as part of an existing research database approval (17/LO/0008).

Data Collection

Routine clinical information was extracted from the institution's Electronic Health Record (EHR) system using a custom structured query language script. These data included demographic information, laboratory results, intraoperative, CPB, and medication administration data, and intensive care requirements. Comorbidities (including risk scores), and outcomes were defined using Association for European Paediatric and Congenital Cardiology coding as part of the institution's NICOR routine data submissions. Intraoperative data from the heart-lung and anaesthetic machines were captured every minute throughout surgery. Preoperative risk estimation was based on cardiac and non-cardiac preoperative risk factors using the Partial Risk Adjustment in Surgery (PRAiS2) model (Rogers et al, 2017). Baseline serum creatinine levels were taken within the 24 hours preceding surgery. Intraoperative blood biochemistry

medRxiv preprint doi: https://doi.org/10.1101/2024.03.18.24304520; this version posted March 19, 2024. The copyright holder for this preprint (which was not certified by peer review) is the author/funder, who has granted medRxiv a license to display the preprint in perpetuity. It is made available under a CC-BY-NC-ND 4.0 International license .

(including haemoglobin, arterial oxygen partial pressure and saturation, and mixed-venous oxygen saturation) was measured continuously using an optical fluorescence and reflectance system (CDI550, Terumo, Leuven, Belgium), calibrated every 20 minutes using a cassette-based blood gas analyzer (ABL90 Flex Plus, Radiometer, Copenhagen, Denmark). HLM variables were automatically recorded in one minute intervals via a bidirectional connection into the Institutional EHR system (Axon, Philips Capsule, Paris, France). Postoperative Acute Kidney Injury (AKI) was calculated according to the Kidney Disease Improving Global Outcomes (KDIGO) criteria (Khwaja, 2012), based on the patients' serum creatinine change and urine levels within the first 48 hours following surgery. Patients were assigned the highest AKI grouping on the basis of these two criteria. The final KDIGO score for each patient is an integer between 0 (no AKI) and 3 (severe AKI).

Anaesthesia

Anesthesia was induced by inhalation of sevoflurane in oxygen and, after induction, fentanyl 5 mg/kg and pancuronium100 mg/kg were given; maintenance was with isoflurane 1.0% in oxygen and air. After tracheal intubation, arterial and central venous lines were inserted. Further incremental doses of fentanyl, up to 25 mg/kg, were given during the procedure.

CPB

The CPB circuit consisted of FX oxygenators with integrated arterial line filter and hard-shell venous reservoir (Terumo Corp). The Stöcket S5 (Stöcket, LivaNova) heart-lung machine with pole-mounted roller pumps was used with a 3T heater/chiller (Stöcket, LivaNova). The total base prime volume was 330 - 1000 mL depending on circuit size. When the predicted initial CPB hematocrit was <27% the prime consisted of packed red blood cells of the patient's blood group (120-200 mL), a synthetic colloid (Gelofusine; B Braun Melsungen AG), heparin 1000 U/mL, 1.5 mL (Heparin Sodium; Wockhardt). Blood primed circuits were then washed with 1000 mL of balanced crystalloid solution (Plasmalyte 7.4; Baxter) by performing prebypass ultrafiltration, carried out as previously described, to ensure an initial on-CPB hematocrit of 30% (Naik

medRxiv preprint doi: https://doi.org/10.1101/2024.03.18.24304520; this version posted March 19, 2024. The copyright holder for this preprint (which was not certified by peer review) is the author/funder, who has granted medRxiv a license to display the preprint in perpetuity. It is made available under a CC-BY-NC-ND 4.0 International license .

and Elliott, 1993). Biochemical compatibility was then attained using sodium bicarbonate as a buffering agent. Patients requiring a clear prime received crystalloid and colloid volumes in a 40:60 mix, with 10 mL sodium bicarbonate and 2 to 5 mL heparin. All patients were systemically cooled to nasopharyngeal temperatures between 28 and 35°C unless undergoing deep hypothermic circulatory arrest, in which case the patient was cooled to 18°C. Myocardial protection was achieved with 30 mL/kg of cold blood cardioplegia (4:1 blood:cardioplegia to a final concentration of 20 mmol) of St Thomas's Solution (IVEX Pharmaceuticals). During the rewarming phase of CPB, a gradient no greater than 10°C between the patient's nasopharyngeal temperature probe and the heater/chiller (maximum arterial blood temperature 37.5°C) was maintained until a maximum oesophageal temperature of 36°C was achieved.

Data Preparation

All data preparation and analysis for this research has been conducted using the R programming language and its various packages (R Core Team, 2021).

Data Cleaning

Each operation was split into one or more 'sessions' of contiguous timestamps (every minute). After calculating the necessary derived fields (see below), a boolean 'validity' flag was calculated for each intraoperative recording, enforcing the following conditions: $0 < Hct < 0.6$, $0 \leq SvO_2 \leq 100$, $SvO_2 < SaO_2$, $T > 0$, $CI > 0$, where CI is cardiac index (blood flow indexed to BSA) in L/min/m^2, Hb is blood haemoglobin level in g/dL, and SaO_2 is the haemoglobin oxygen saturation of arterial blood, expressed as a percentage. (The last condition removes periods of DHCA, i.e., $CI = 0$, from further analysis.) Also, we flag any recordings with missingness as invalid, thus limiting our time-series analysis to valid 'segments' created within each session.

In calculating the change terms used for constructing the design matrix of the GARIX+ model (Equation 9), we impose a minimum segment length of 10 minutes for the GARIX+(7) model, and 25 minutes for the GARIX+(20) model. When comparing

medRxiv preprint doi: https://doi.org/10.1101/2024.03.18.24304520; this version posted March 19, 2024. The copyright holder for this preprint (which was not certified by peer review) is the author/funder, who has granted medRxiv a license to display the preprint in perpetuity. It is made available under a CC-BY-NC-ND 4.0 International license .

GARIX+ models of different N, we used a single value for the minimum segment length to prepare a common dataset.

Derived Fields

Body surface area (BSA) is defined according to the Monsteller formula:

$$BSA = \sqrt{\frac{Height \times Weight}{3600}}, \quad (1)$$

where height is in cm, and weight is in kg.

Oxygen delivery (indexed to BSA) is given by:

$$DO_2i = CI \times Hb \times 1.36 \times (SaO_2/100) \times 10, \quad (2)$$

In the above equation, the contribution to oxygen content of blood from dissolved oxygen is ignored, thus focusing exclusively on the haemoglobin-bound oxygen. (In our data, dissolved oxygen constitutes only 1.6% of total oxygen content in arterial blood, thus supporting the plausibility of ignoring the dissolved-oxygen component in our analysis.)

Similarly, for oxygen consumption:

$$VO_2i = CI \times Hb \times 1.36 \times ((SaO_2 - SvO_2)/100) \times 10, \quad (3)$$

where, again, the contribution from change in the dissolved oxygen content of the blood is ignored. This allows us to write OER as:

$$OER = \frac{VO_2i}{DO_2i} = \frac{SaO_2 - SvO_2}{SaO_2}, \quad (4)$$

Therefore, VO_2i can be rewritten as:

$$VO_2i = CI \times Hb \times 1.36 \times (SaO_2 / 100) \times 10 \times OER. \quad (5)$$

Kirklin Equation

The following equation (page 119 of Kirklin and Blackstone, 2012) represents a hyperbolic functional form for dependence of VO_2i on CI (and ultimately on DO_2i), along with a Van't Hoff dependence of tVO_2i on temperature (T):

$$1 / VO_2i = 0.168 \times 10^{-0.0387 \times T} + 0.0378 \times 10^{-0.0253 \times T}/CI. \quad (6)$$

medRxiv preprint doi: https://doi.org/10.1101/2024.03.18.24304520; this version posted March 19, 2024. The copyright holder for this preprint (which was not certified by peer review) is the author/funder, who has granted medRxiv a license to display the preprint in perpetuity. It is made available under a CC-BY-NC-ND 4.0 International license .

Comparing the above to the equation of Figure 1, we see that, according to Equation 6, we must have $tVO_2i = (1/0.168) \times 10^{0.0387T}$, implying a Q10 of $10^{10\times0.0387} = 2.44$.

The GARIX+ Time-Series Model

The main assumption of the model is that changes (from one minute to the next) in the 'logit' of OER follow a homoscedastic (fixed-variance) normal distribution, and the distribution mean is a linear function of three 'term groups' (TGs): the disequilibrium TG (DTG), the autoregressive TG (ATG), and the exogenous TG (ETG). As a reminder, the logit transformation is given by:

$$logit(x) = \log(\frac{x}{1-x}). \tag{7}$$

It is useful for mapping a variable with a range between 0 and 1 (such as OER) to an unbounded range of $-\infty$ to $+\infty$, making it a more natural fit for linear models. The model, therefore, reads:

$$logit(OER)_{t+1} - logit(OER)_t \sim N(\mu_t, \sigma^2), \tag{8}$$

where the subscripts indicate measurement times (in minutes), N is the univariate normal (or Gaussian) distribution, μ_t is the time-dependent mean of the normal distribution, and σ^2 is the time-independent variance of the distribution. The distribution mean at time t, μ_t, is given by:

$$\begin{aligned}
&\mu_t = \\
\text{DTG} \longrightarrow\ & -k(\log(VO_2i)_t - \log(tVO_2i)_t) + \\
\text{ATG} \longrightarrow\ & \sum_{n=1}^{N} \beta_n(logit(OER)_{t-(n-1)} - logit(OER)_{t-n}) + \\
\text{ETG}\ \Bigg\{\ & \sum_{n=0}^{N} \gamma_{1,n}(\log(CI)_{t-(n-1)} - \log(CI)_{t-n}) + \sum_{n=0}^{N} \gamma_{2,n}(\log(Hb)_{t-(n-1)} - \log(Hb)_{t-n}) + \\
& \sum_{n=0}^{N} \gamma_{3,n}(\log(SaO_2)_{t-(n-1)} - \log(SaO_2)_{t-n}) + \sum_{n=0}^{N} \gamma_{4,n}(T_{t-(n-1)} - T_{t-n}).
\end{aligned} \tag{9}$$

medRxiv preprint doi: https://doi.org/10.1101/2024.03.18.24304520; this version posted March 19, 2024. The copyright holder for this preprint (which was not certified by peer review) is the author/funder, who has granted medRxiv a license to display the preprint in perpetuity. It is made available under a CC-BY-NC-ND 4.0 International license .

The convention GARIX+(N) is used to refer to a GARIX+ model with a history length of N according to Equation 9. Also note that we have used the log transformation for state variables, CI, Hb and $SaO2$ in order to reduce their skewness.

Below we discuss each of the three TGs in the GARIX+ model. A conceptual summary of the model is provided in Figure 2.

Disequilibrium Term Group (DTG)

The DTG represents a force to move OER in such a direction as to make VO_2i equal to tVO_2i. For this interpretation to be sensible, the parameter 'k' - which we refer to as the 'disequilibrium coefficient' - is expected to be positive: For instance, when VO_2i is larger than tVO_2i (over-oxygenation), then $\log(VO_2i_t) - \log(tVO_2i_t)$ would be positive, and hence $-k(\log(VO_2i_t) - \log(tVO_2i_t))$ would be negative (assuming $k > 0$). This induces a negative change in logit(OER), i.e., a decrease in OER, which would result in reduced VO_2i, thus bringing it closer to tVO_2i. The reverse would happen if VO_2i is smaller than tVO_2i (under-oxygenation).

Assuming that oxygen demand (tVO_2i) follows the Van't Hoff parametric form, we have:

$$\log(tVO2i) = \alpha_0 + \alpha_1 T \tag{10}$$

From the above, Q10 can be readily calculated:

$$Q_{10} = \frac{tVO_2i(T+10)}{tVO_2i(T)} = \frac{\exp(\alpha_0+\alpha_1(T+10))}{\exp(\alpha_0+\alpha_1 T)} = \exp(10\,\alpha_1). \tag{11}$$

Combining Equations 9 and 10, the following expression for DTG is obtained:

$$DTG = -k\,(\log(VO_2i) - \alpha_0 - \alpha_1 T) \tag{12}$$

Since the above specification isn't suitable for linear regression, we switch to the conventional specification:

$$DTG = \eta_0 + \eta_1 \log(VO_2i) + \eta_2 T, \tag{13}$$

which can be converted back to Equation 12 using:

$$k = -\eta_1,\ \alpha_0 = -\eta_0/\eta_1,\ \alpha_1 = -\eta_2/\eta_1. \tag{14}$$

Note that the above transformations are nonlinear, which means for estimating confidence intervals for k, α_0, α_1, we use Monte Carlo simulations, where samples are

medRxiv preprint doi: https://doi.org/10.1101/2024.03.18.24304520; this version posted March 19, 2024. The copyright holder for this preprint (which was not certified by peer review) is the author/funder, who has granted medRxiv a license to display the preprint in perpetuity. It is made available under a CC-BY-NC-ND 4.0 International license .

drawn from the joint normal distribution on (η_0, η_1, η_2), returned by linear regression software in R, and k, α_0, α_1 within each sample are computed according to Equations 14.

Exogenous Term Group (ETG)

The ETG represents the effect of intended changes (the $n = 0$ terms in Equation 9) and past changes (the $n > 0$ terms in Equation 9) in the exogenous state variables ($\log(CI)$, $\log(Hb)$, $\log(SaO_2)$, T) on change in $logit(OER)$. Larger n's correspond to more distant pasts. See Limitations for a discussion of endogeneity vs. exogeneity of state variables.

Autoregressive Term Group (ATG)

The ATG represents the force that previous changes in OER exert on its future trajectory. Each term in this TG, $\beta_n(logit(OER)_{t-(n-1)} - logit(OER)_{t-n})$, corresponds to the change in logit(OER) from time $t - n$ to time $t - (n - 1)$, i.e., n minutes ago (since t represents 'present' time). If the coefficient, β_n, is negative, this term would produce a 'self-correcting' force, i.e., reversing stochastic changes in OER. For instance, if $\beta_1 < 0$, then an increase in OER during $t -> t + 1$ would produce a force that seeks to reduce OER from $t + 1$ to $t + 2$.

When equilibrium is changed, for example due to cardiac index changing without any concomitant change in temperature, the force produced by the DTG is partially negated by the ATG contribution (Figure 3E). Note that ATG does not include an 'intended' term, i.e., $n = 0$, since this change corresponds to the outcome (endogenous) variable, which is not known at the time of making the prediction; rather, the change in logit(OER) from t to $t + 1$ is exactly what is being predicted.

Static Model

As a reference point for the dynamic model, a naive, static model for learning the dependence of tVO_2i on temperature is considered. In this static model, an assumption is made that VO_2i is simply equal to tVO_2i at all times; in other words, both supply constraints and system dynamics are ignored. The relationship between tVO_2i and

medRxiv preprint doi: https://doi.org/10.1101/2024.03.18.24304520; this version posted March 19, 2024. The copyright holder for this preprint (which was not certified by peer review) is the author/funder, who has granted medRxiv a license to display the preprint in perpetuity. It is made available under a CC-BY-NC-ND 4.0 International license .

temperature is again assumed to follow the Van't Hoff specification, as in the dynamic model. This leads to the following regression model:

$$\log(VO_2i_t) \sim N(\beta_0 + \beta_1 T_t, \sigma^2) \quad (15)$$

which can be readily estimated from the perfusion data.

Variable Importance Analysis

For Variable Importance (VI) analysis, a permutation-based method is used (Altmann et al, 2010), embedded in a repeated cross-validation (CV) scheme. In our context, the goal in conducting VI analysis is to quantify the relative importance of different variables, rather than variable selection. Permutation-based VI (PVI) is a model-agnostic VI method that measures degradation in predictive accuracy caused by random shuffling of the column (or columns) of the design matrix corresponding to the variables(s) in consideration. PVI is embedded in repeated cross-validation, in order to base the performance change on out-of-sample - rather than in-sample - predictive accuracy. Note that random shuffling applies not to the original time-series data but to the transformed version of the data that is used in estimating the linear regression coefficients. Relatedly, when applying PVI to TGs, the same random reordering of rows is applied to all individual terms in a TG (with each term corresponding to a column in the design matrix).

System Simulations

Simulations are conducted to illustrate system response to exogenous changes. They can be done in two modes: deterministic and stochastic. In deterministic mode, the change in $logit(OER)$ from time t to time $t + 1$ is taken to be the predicted mean, μ_t. In stochastic mode, the predicted mean is added to a random deviate drawn from a normal distribution with variance equal to σ^2, which is estimated during model training. Unless mentioned explicitly otherwise, initial conditions for simulations were based on median values of exogenous variables (ci, Hb, $SaO2$ and T) in the training data, and OER was calculated, using the GARIX+ model, such that the system would be in equilibrium (DTG = 0), where DTG is given by Equation 12.

medRxiv preprint doi: https://doi.org/10.1101/2024.03.18.24304520; this version posted March 19, 2024. The copyright holder for this preprint (which was not certified by peer review) is the author/funder, who has granted medRxiv a license to display the preprint in perpetuity. It is made available under a CC-BY-NC-ND 4.0 International license .

Results

Patients and Outcomes

Table 1 shows a summary of patients used in the study and their outcomes. Note that, aside from gender and ethnicity, all other variables are per-operation. For instance, if a patient has had multiple operations, their age at the beginning of each operation is entered into the calculations. With regards to mortality, we see the observed 30-day mortality rate in our dataset is slightly below the expected mortality rate - for the same operations - calculated according to the PRAiS2 protocol.

GARIX+ Model Fit

Figure 3 shows the results of fitting the above-described GARIX+ model to the granular perfusion data. The magnitude of coefficients for autoregressive and exogenous terms declines with lag increase and reaches statistically insignificant levels after 10 minutes or so, consistent with a finite memory in the system (Panel A). (See Supp Mat E for the complete list of coefficients for the GARIX+(20) model.) Coefficient signs are consistent with an adaptive OER change to: 1) maintain oxygen consumption at a fixed temperature (negative coefficients for change terms involving $\log(CI)$ and $\log(Hb)$); 2) increase/decrease oxygen consumption when temperature is increased/decreased, respectively (positive coefficients for change terms involving T); and 3) stabilise random fluctuations in oxygen consumption (negative coefficients for $logit(OER)$ change terms). SaO_2 is a special case since it is also part of the OER definition: $OER = 1 - SvO_2/SaO_2$, and it therefore influences VO_2i both directly, and also via OER:

$$VO_2i = CI \times Hb \times 1.36 \times (SaO_2 / 100) \times 10 \times OER.$$

As shown in Methods, the DTG coefficients can be used to calculate Q10 and construct the Van't Hoff curve (Panel B). The estimated Q10 is 2.2, which is close to the 2.4 figure given in Kirklin & Blackstone (2012), and significantly below the 3.7 value estimated from the data using a naive, i.e. static, model (see Static Model). Also, 'k', the disequilibrium coefficient, is estimated to be 0.024, with a 95% confidence interval of 0.021-0.026 that is significantly positive. Positivity of the disequilibrium coefficient is consistent with an adaptive force to bring VO_2i in line with target VO_2i.

medRxiv preprint doi: https://doi.org/10.1101/2024.03.18.24304520; this version posted March 19, 2024. The copyright holder for this preprint (which was not certified by peer review) is the author/funder, who has granted medRxiv a license to display the preprint in perpetuity. It is made available under a CC-BY-NC-ND 4.0 International license .

By construction, the static fit assumes that the data is balanced between episodes of under- and over-oxygenation. (Note, however, that the static regression is performed on the logarithm of VO_2i, which means residuals may not be balanced on the original scale, especially if the model is misspecified.) Yet, within each subject, and especially at the granular, minute-by-minute level, there are significant deviations from the regression line, as can be seen in Figure 3B. On the other hand, the GARIX+(7) fit implies more cases of over-oxygenation, especially at higher temperatures. While the 'Kirklin - asymptote' line has a Q10 close to GARIX+, the absolute levels are significantly higher. The discrepancy becomes smaller when we use the 'clinical' values given in Figure 2-11 of Kirklin and Blackstone (2012). Either way, the Kirklin lines imply under-oxygenation to be a more prominent risk, compared to the fit obtained from our GARIX+ model.

Panel C confirms that only 5-10 minutes of history are useful for improving the out-of-sample predictive accuracy of the model. This observation is the basis for using GARIX+(7) in most of the remaining analyses in this paper. It is possible, however, that larger training data would justify using a longer history.

Panel D shows PVI by TGs (DTG, ATG, and ETG). Note that DTG - which allows the estimation of tVO_2i and its dependence on temperature - has the smallest, but statistically significant, contribution of the three TGs. This limits the ability to conduct subgroup analyses, and to include many patient attributes and interaction terms in the DTG of the model.

Panel E shows the timeline of contributions from different TGs to change in $logit(OER)$, driven by a hypothetical step-function change in CI at t = 0. The initial, fast adaptation is dominated by the ETG, while the secondary, slow adaptation is dominated by the counteracting effects of the DTG and the ATG. The ATG contribution (red) is partially offsetting the DTG (green), resulting in a slower overall adaptation rate (purple). Panel F illustrates the resulting OER trajectory consisting of the initial fast stage, followed by the secondary, slow stage.

medRxiv preprint doi: https://doi.org/10.1101/2024.03.18.24304520; this version posted March 19, 2024. The copyright holder for this preprint (which was not certified by peer review) is the author/funder, who has granted medRxiv a license to display the preprint in perpetuity. It is made available under a CC-BY-NC-ND 4.0 International license .

Subgroup Analysis by KDIGO Score

Next, we trained the GARIX+(7) model on subsets of patients that all share a single KDIGO score. Comparing these models allows us to identify interesting correlates of AKI severity.

In Panel A of Figure 4, the model fit, measured by the out-of-sample (OOS) R-squared, degrades with increased AKI severity (i.e., increasing KDIGO score; red line labelled 'Genuine'), and this decline cannot be explained by changes in the sample size (blue line, labelled 'Random'). This is directionally consistent with the model reflecting, at least to some degree, normal body mechanisms (which would presumably be stronger in AKI-free patients), rather than a purely pathological set of interactions triggered by the extreme conditions that patients undergo during CPB.

Panel B shows that the immediate adaptive reaction to changes in haemoglobin is an important factor in explaining the change in model performance with AKI: Those with severe AKI show a much less pronounced immediate adaptation to a change in blood haemoglobin levels. Also, as panel C shows, the disequilibrium force becomes steadily weaker (smaller disequilibrium coefficient or 'k') in patients with more severe AKI, which is, in turn, reflected in a slower adaptation time (Panel D). Finally, smaller Q10 values in higher-KDIGO patients (corresponding to the α_1 parameter in Panel C) suggests a weaker dependence of metabolic needs - genuine or pathological - on body temperature in severe-AKI cases.

Comparison to the Kirklin Model

The elbow, or piecewise linear, model - where VO_2i becomes completely supply-independent after DO_2i exceeds a threshold - is appealing due to its simplicity, and also because it provides exact estimates not only for tVO_2i, but also for tDO_2i. However, empirical evidence (Kirklin & Blackstone, 2012) suggests that a hyperbolic model of oxygen consumption is more accurate in explaining the - albeit limited and dated - human and animal data.

The GARIX+ dynamic model offers an alternative explanation of empirical data. Figure 5 shows the results of simulating the human experiments reported by Fox et al (1982).

medRxiv preprint doi: https://doi.org/10.1101/2024.03.18.24304520; this version posted March 19, 2024. The copyright holder for this preprint (which was not certified by peer review) is the author/funder, who has granted medRxiv a license to display the preprint in perpetuity. It is made available under a CC-BY-NC-ND 4.0 International license .

With a wait time of 10 minutes between state transitions, GARIX+(7) model produces a DO_2i-VO_2i curve that is similar to the hyperbolic fit of Kirklin. As wait time is increased, the GARIX+(7) model produces sharper curves, and at infinity it converges to the piecewise linear shape. As shown earlier (Figure 3B), the predicted tVO_2i is higher in Kirklin than GARIX+(7) at all temperatures. As shown in Table 2, the distributions of R-squared, 'a' and 'b' parameters (using Fox et al convention, see Supp Mat B) according to GARIX+(7) - and using a wait time of 10 minutes between state transitions - all have 95% confidence intervals that cover the results reported in Fox et al.
While a static view of the piecewise linear model would only allow for the possibility of under-oxygenation, the shift to a dynamic perspective opens up both possibilities. This is illustrated in Figure 6, which shows a 3D surface plot of oxygenation gap (OG) (y axis) vs. the relative step change in DO_2i at t = 0 (x axis), and at different times since the introduction of step change (z axis). OG is defined as the % difference between oxygen consumption at time t (VO_2i_t), and target oxygen consumption (tVO_2i):
$OG_t = 100 \times (VO_2i_t - tVO_2i) / tVO_2i$. (Note that tVO_2i does not change with time since temperature is fixed.) It can be demonstrated that, for small t's, the response is nearly linear, corresponding to relatively little adaptation in OER. This means that, e.g., when cardiac index is increased and before OER adaptively decreases to bring VO_2i down to its pre-perturbation level, there will be a nearly proportional oxygen consumption surplus, or over-oxygenation. However, as time progresses, such oxygen surplus dissipates as OER adaptively decreases. While oxygen surplus eventually vanishes, oxygen deficit cannot completely disappear if the ratio $tVO2i/DO2i$ implies an OER greater than 1. As a result, the piecewise linear shape emerges for very large t's.

Q10 by Temperature Band

One of the limitations of the Kirklin model (Equation 6) is that the dependence of tVO_2i on temperature was assumed to follow the strict parametric form of Van't Hoff (where the logarithm of oxygen demand is a linear function of temperature), and yet the evidence for this strong parametric assumption is scant. In fact, Equation 6 is based only on two data points: a set of human experiments conducted in 1982 at 20℃ (Fox et

medRxiv preprint doi: https://doi.org/10.1101/2024.03.18.24304520; this version posted March 19, 2024. The copyright holder for this preprint (which was not certified by peer review) is the author/funder, who has granted medRxiv a license to display the preprint in perpetuity. It is made available under a CC-BY-NC-ND 4.0 International license .

al, 1982), and three sets of animal experiments conducted in the 1950s, at 37℃ (Cheng et al, 1959; Paneth et al, 1957; Starr, 1959). While the Van't Hoff specification has been followed in Equation 9 due to its widespread adoption, it may be informative to perform a subgroup analysis by temperature in order to see if the GARIX+(7) model arrives at the same, or close values of Q10 within different temperature bands.

As Figure 7A shows, most of the temperature recordings are clustered in the 30-37℃ range. This, combined with a low relative VI for the DTG means that models trained within fine temperature subgroups may not yield statistically significant results for the parameters of DTG. Therefore, we opted to create two temperature bands, separated at 28℃ (Panel B). We observe that, GARIX+(7) models that are fit within each subgroup yield significantly different oxygen demand curves. While the low-temp regime has a Q10 of 2.6, the high-temp regime produces a Q10 that is barely above 1, suggesting a much less pronounced dependence of oxygen demand on temperature in this range.

Discussion

This study is the first to present a data-driven, analytical framework for predicting OER changes in response to clinical interventions during CPB. The analysis was made possible through a combination of granular perfusion data, combined with two important methodological enhancements to an otherwise standard framework for time-series analysis.

Our model suggests that changes in the components of oxygen delivery cause an adaptive OER response to keep oxygen consumption in line with oxygen demand, according to body temperature. The dependence of oxygen demand on temperature decreases as temperature increases towards normothermia, calling into question the accepted Van't Hoff equation. Children developing AKI exhibit a dampened response to changes in haemoglobin during CPB, with this dampening of response intensifying with AKI severity. This association can be the foundation of an intraoperative tool for early diagnosis of at-risk patients. Furthermore, our model provides a novel framework for GDP by identifying periods of over- and under-oxygenation through comparing the VO_2i against tVO_2i, and by predicting the impact of perfusionist actions on OER and oxygen consumption.

medRxiv preprint doi: https://doi.org/10.1101/2024.03.18.24304520; this version posted March 19, 2024. The copyright holder for this preprint (which was not certified by peer review) is the author/funder, who has granted medRxiv a license to display the preprint in perpetuity. It is made available under a CC-BY-NC-ND 4.0 International license .

GARIX+ as a Grey-Box Model

In creating GARIX+, a standard autoregressive, integrated time-series model with exogenous variables (ARIX) - a black-box model - has been enhanced in two important ways. First, a DTG has been added (hence the '+' sign) that reflects our expectation that the body seeks to keep oxygen consumption in line with its metabolic needs, as dictated by body temperature. Secondly, the data points are combined across all patients, resulting in a 'global' time-series model. This gave the model sufficient statistical power to estimate the DTG parameters, despite their relatively-small VI compared to the ATG and ETG. Within the DTG, the dependence of oxygen demand (tVO_2i) on temperature is assumed to follow the Van't Hoff model, which is the standard specification in the literature. As such, GARIX+ can be characterised as a 'grey-box' model; that is, a black-box model enhanced with domain knowledge.

In a GARIX model (no '+'), any combination of state variables (CI, Hb, SaO_2, OER and temp) would be acceptable as a solution, as long as they all remain constant with time. While a GARIX model could explain much of the OER variations in the data (as evidenced in low relative VI of the disequilibrium TG in Figure 3D), from a physiological perspective it would be an incomplete model since it does not reflect the expectation that the system would seek to adapt oxygen consumption to match the metabolic needs of the body. At the same time, the linear specification of GARIX+, which was our primary reason for not using machine learning models, allowed us to examine and interpret the model coefficients and gain confidence in the physiological plausibility of the results, a topic that is further discussed next.

Physiological Interpretation of Findings

The GARIX+ Model

Oxygen, whilst vital, can also be toxic, with both oxidative stress and cellular hyperoxia identified as major contributors to multiple pathological states (Evans, 2016). Historically, under-oxygenation was (and still remains) the key concern in patients undergoing cardiac surgery, although recent studies are starting to highlight the pathological dangers of over-oxygenation during CPB, with an ongoing debate around

medRxiv preprint doi: https://doi.org/10.1101/2024.03.18.24304520; this version posted March 19, 2024. The copyright holder for this preprint (which was not certified by peer review) is the author/funder, who has granted medRxiv a license to display the preprint in perpetuity. It is made available under a CC-BY-NC-ND 4.0 International license .

the level of damage (Jakutis et al, 2017; Young 2012; Abou-Arab et al, 2020). Equally, being able to define what these terms (over- and under-oxygenation) mean is complex. For example, within the kidney's microcirculation, the renal medulla is normally exposed to lower partial pressures of oxygen compared to the renal cortex, therefore under- and over-oxygenation will be very different conditions, even in the same organ (Evans et al, 2008). Hyperoxia, however, is a phenomenon not encountered in the natural world, and therefore one could speculate that there has been little evolutionary need to develop countermeasures to it (although atmospheric oxygen levels have historically been much higher than they are today; Lane 2003). At the cellular level, oxygen is involved in the final step (Electron Transport Chain, ETC) of aerobic metabolism, in the mitochondria. Whilst the citric acid (Kreb's) cycle will only occur in the presence of oxygen, it will continue even to a mitochondrial PO_2 level as low as 3mmHg (0.4 kPa), with a K_M of 22 mmHg (1.6 kPa; Wilson et al, 2012).

Therefore, an explanation for the piecewise linear model is that once sufficient oxygen molecules are available (oxygen consumption) to support the ETC, further increases in partial pressure will not increase the rate of metabolism. Moreover, as oxygen concentrations reach excessive levels, animal and cell culture models have demonstrated diminished ETC function and altered mitochondrial morphology (Resseguie et al, 2015). Paradoxically, hypoxia is also associated with an increased release of Reactive Oxygen Species (ROS) and mitochondria themselves appear to be O_2 sensing although our understanding of the mechanisms behind this is still incomplete (Guzy and Schumacker, 2006). Hence, there are clear indications that a balance in oxygen consumption and extraction is playing out at the cellular level, and supports our notion for a Disequilibrium Term Group at the systemic level; i.e., the body is attempting to maintain VO_2 in line with tVO_2. Given that individual tissues and organs are known to operate at varying PaO_2 levels or with different metabolic requirements, and even require particular OER levels to maintain proper concentration gradient of oxygen, it follows that, at a systemic level, alterations to exogenous variables (represented in the Exogenous Term Group in the model) will have shorter or longer effects in those tissues (Wolff, 2013). This lag or memory of previous events may be also partially a result of perfusionist interventions coming in relatively rapid succession and independently of

medRxiv preprint doi: https://doi.org/10.1101/2024.03.18.24304520; this version posted March 19, 2024. The copyright holder for this preprint (which was not certified by peer review) is the author/funder, who has granted medRxiv a license to display the preprint in perpetuity. It is made available under a CC-BY-NC-ND 4.0 International license .

normal physiological mechanisms. Such deviations from the normal autoregulatory patterns are frequently seen during CPB, and indeed, a recent review indicated that cardiac surgery is associated with changes in cerebral autoregulation which significantly relate to clinical outcomes (Caldas et al, 2018).

Dependence of Q10 on Temperature Regime

Oxygen can regulate glycolysis via the Pasteur effect. The availability of oxygen will suppress glycolysis, and decreased availability leads to an acceleration of glycolysis, at least initially. This appears to be regulated by several factors including the allosteric regulators of glycolysis (enzymes such as hexokinase; Lenzen 2014).

Allosteric enzymes do not follow the Van't Hoff dependence on temperature, instead often displaying a sigmoid shape for dependence of reaction velocity on temperature, at a fixed substrate concentration.

Whilst Q10 has been traditionally used to describe the dependence of rate of chemical reactions on temperature, enzymatic reactions have ranges over which the proteins can operate before conformational changes or denaturing occurs. Furthermore, bypass physiology is very different from normal human physiology, in that exogenous variables (such as haemoglobin concentration, cardiac index etc.) are manipulated separately by the perfusionist, rather than in coordination, as would be under normal biology. For instance, normal physiological mechanisms to combat hypothermia (such as shivering) are prevented through general anaesthesia, and PaO_2 is managed at levels higher than observed naturally, in order to allow a margin of safety. In the analysis described in this study, a lower Q10 value was measured in patients that were treated with mild hypothermia (>28℃), compared to those with moderate and deep hypothermia (<28℃). One might postulate that under mild hypothermic conditions sufficient substrate and oxygen is being provided, and enzymatic functions are maintained such that they lead to a degree of decoupling between metabolic rate and temperature. On cooling further into moderate and deep hypothermia, this independence is lost and we thus return to the more traditional Q10 of 2-3. However, further, independent data are required to validate these observations and experimentation is needed to determine the cellular mechanisms operating in different temperature regimes.

medRxiv preprint doi: https://doi.org/10.1101/2024.03.18.24304520; this version posted March 19, 2024. The copyright holder for this preprint (which was not certified by peer review) is the author/funder, who has granted medRxiv a license to display the preprint in perpetuity. It is made available under a CC-BY-NC-ND 4.0 International license .

Altered Model Performance in Patients Developing AKI

The aetiology of AKI is complex and incompletely understood. Some studies have pointed to renal haemodynamics and oxygenation as AKI triggers (Evans et al., 2018), whilst a meta-analysis suggested hypertension, alterations of serum creatinine, CPB and aortic clamping times (among others), as strong predictors for the development of postoperative AKI (Yi et al 2016). Renal oxygenation is directly dependent on renal blood flow and its regulation, and its oxygen consumption levels are primarily driven by tubular demand, which itself is dependent on the glomerular filtration rate (Smith et al 1940). There exist, within the kidney, regional variations in oxygen delivery and consumption; areas with normally lower physiological pO_2 are at greater risk of hypoxic damage through alterations in the delivery - consumption balance (Edwards and Kurtcuoglu, 2022).

The reduced performance of the GARIX+ model in severe AKI patients, as well as their slower adaptation seems physiologically plausible, as it suggests a disruption of feedback pathways in severe-AKI patients. The causality mechanism is not clear, however. For instance, slower adaptation may be causing AKI by creating prolonged periods of imbalance between oxygen consumption and demand, or there may be a common cause for slower OER adaptation during CPB, and postoperative AKI. One of the limitations of this (and indeed nearly every other) study examining AKI after CPB, is a lack of direct measurement of blood flow and oxygenation occurring in the kidney. Therefore it is impossible to provide a definitive explanation for the slowing of the adaptive response in high-severity AKI patients (Figure 4D). However, this is consistent with an exaggerated supply-dependence of consumption in critically-ill patients, including those with sepsis (Friedman et al, 1998).

An intriguing observation from the GARIX+ model, is the decline in adaptive response to haemoglobin changes in severe-AKI patients. Furthermore, although not detailed in this manuscript, a progressively weaker haemoglobin response was observed in younger patients. During CPB, other than through haemofiltration, the only way to increase Hb concentration is through the addition of stored RBCs. Due to the large volume of the CPB circuit relative to the child's circulating volume, RBC transfusions are more common in paediatric than adult surgery. A recent study examined the effect of RBC

medRxiv preprint doi: https://doi.org/10.1101/2024.03.18.24304520; this version posted March 19, 2024. The copyright holder for this preprint (which was not certified by peer review) is the author/funder, who has granted medRxiv a license to display the preprint in perpetuity. It is made available under a CC-BY-NC-ND 4.0 International license .

transfusion on renal oxygenation in kidneys supported via an *ex vivo* normothermic kidney perfusion rig (Bumbill et al 2023). It demonstrated that there was slower O_2 unloading from stored RBC with concomitant reduction in O_2 extraction in perfused kidneys, indicating diffusion-limited O_2 release at capillaries. It is also possible that SaO_2 dependence on PaO_2 - i.e. the oxygen dissociation curve - shifts differently with transfused RBC's due to the metabolic and morphological changes that can occur due to storage (Bennett-Guerrero, 2007 & Yoshida, 2019). Further examination is required to ascertain the underlying mechanism for this response, but it presents a potential mechanism for early - i.e., intraoperative - diagnosis of patients at risk of post-surgical AKI.

Implications for Goal-Directed Perfusion

Whilst the majority of research has focused on preventing under-oxygenation of the tissues during CPB, little has been done to date to assess over-oxygenation. Furthermore, DO_2i provides limited information and assumes an optimised dissociation curve occurring across all tissues. Using predicted tVO_2i as a reference (see Table 3) will allow the more specific definition of over-and under-oxygenation, increasing the predictive power towards AKI and other adverse events.

Limitations

Contribution from dissolved oxygen

The contribution from dissolved oxygen was not considered due to a lack of access to PvO_2 (partial pressure of mixed venous oxygen). However, as stated before, this contribution is on average only around 1.5% of the total oxygen content. Therefore, the analysis and results can be considered directionally correct. Future work will incorporate the dissolved-oxygen component and improve the accuracy of the models.

Endogeneity vs. Exogeneity of State Variables

Exogeneity of CI, Hb, SaO_2 is an idealised assumption. In reality, values of these state variables at time "t+1" cannot be set with full certainty at time "t"; rather, these variables

medRxiv preprint doi: https://doi.org/10.1101/2024.03.18.24304520; this version posted March 19, 2024. The copyright holder for this preprint (which was not certified by peer review) is the author/funder, who has granted medRxiv a license to display the preprint in perpetuity. It is made available under a CC-BY-NC-ND 4.0 International license .

are controlled indirectly. In other words, the boundary between exogeneity and endogeneity is blurred. In particular, SaO_2 is controlled via PaO_2 (changing the arterial oxygen pressure). A basic dynamic model confirmed that PaO_2 (plus temperature) can predict changes in SaO_2 with good accuracy (results not shown here). In future work, more realistic models will be needed to better reflect the true controllability of the 'exogenous' variables.

Constraints on OER

Other than using a logit transformation to implicitly constrain OER to fall between 0 and 1, there were no other constraints on OER. The nonlinearity of the logit transformation also provides a natural slowing down of OER change as it approaches extreme values, which lends further physiological plausibility to the system simulations. It is possible that, during normal conditions, the body deploys other adaptive mechanisms, which may or may not be disrupted during CPB, to ensure that OER remains within a tighter range. During CPB, on the other hand, perfusionists generally go to great lengths to ensure that OER does not stray too far from an acceptable range. For instance, in our data, 90% of time OER remains below 31%. As such, during system simulations, care must be taken while interpreting results where simulated OER approaches or exceeds the observed range in our data.

Paediatric patients

This dataset contains a broad paediatric age range and yet no adults. Mixing neonates and teenagers, who may have very different physiology and different responses in terms of their adaptation to CPB stresses, is not ideal. However, due to the relatively low VI for the DTG (OER variations are dominated by exogenous and autoregressive forces during CPB), we decided to combine all patients to build a single, global model in order to maximise the study power with regards to the steady-state analysis (dependence of tDO_2i on temperature). More data and analyses are needed to differentiate between age groups.

medRxiv preprint doi: https://doi.org/10.1101/2024.03.18.24304520; this version posted March 19, 2024. The copyright holder for this preprint (which was not certified by peer review) is the author/funder, who has granted medRxiv a license to display the preprint in perpetuity. It is made available under a CC-BY-NC-ND 4.0 International license .

Conclusion

This study proposes a physiologically plausible model of OER changes during CPB that is consistent with past experimental data. While in the long-term under-oxygenation is the dominant risk, slow adaptation of OER during CPB creates short-term opportunities for over-oxygenation after significant changes in the exogenous variables, such as a sudden increase in cardiac index. The model provides well-defined values for tVO_2i at a given temperature (Table 3), paving the way for further research into the effects of over- and under-oxygenation on postoperative outcomes such as AKI, and hence improvements in GDP protocols. Furthermore, the identification of an altered response to haemoglobin changes in patients that proceed to severe post-surgical AKI suggests a potential intraoperative diagnostic tool for early identification of at-risk patients.

References

1. O. Abou-Arab, P. Huette, M. Guilbart, H. Dupont and P.-G. Guinot Hyperoxia during cardiopulmonary bypass does not increase respiratory or neurological complications: a post hoc analysis of the CARDIOX study. British Journal of Anaesthesia 2020 Vol. 125 Issue 5 Pages e400-e401.
2. Altmann, André, et al. "Permutation importance: a corrected feature importance measure." Bioinformatics 26.10 (2010): 1340-1347.
3. Bennett-Guerrero, E. et al. Evolution of adverse changes in stored RBCs. Proc Natl
   Acad Sci U S A 104, 17063-17068 (2007).
4. Caldas, J.R., Haunton, V.J., Panerai, R.B., Hajjar, L.A., and Robinson, T.G. Cerebral autoregulation in cardiopulmonary bypass surgery: a systematic review, Interactive CardioVascular and Thoracic Surgery, 2018 26(3) 494–503.
5. Cheng, Huan-Chen, et al. "A study of oxygen consumption during extracorporeal circulation." ASAIO Journal 5.1 (1959): 273-278.
6. Do-Nguyen, Chi Chi, et al. "Oxygen Delivery Thresholds During Cardiopulmonary Bypass and Risk for Acute Kidney Injury." The Annals of Thoracic Surgery (2023).

medRxiv preprint doi: https://doi.org/10.1101/2024.03.18.24304520; this version posted March 19, 2024. The copyright holder for this preprint (which was not certified by peer review) is the author/funder, who has granted medRxiv a license to display the preprint in perpetuity. It is made available under a CC-BY-NC-ND 4.0 International license .

7. Dreher, Molly, et al. "Indexed oxygen delivery during pediatric cardiopulmonary bypass is a modifiable risk factor for postoperative acute kidney injury." The Journal of ExtraCorporeal Technology 55.3 (2023): 112-120.
8. Richard Dumbill, Julija Rabcuka, John Fallon, Simon Knight, James Hunter, Daniel Voyce, Jacob Thomas Barrett, Matt Ellen, Annemarie Weissenbacher, Tetuko Kurniawan, Slawomir Blonski, Piotr M Korczyk, Rutger Jan Ploeg, Constantin Coussios, Peter Friend, Pawel Swietach; Impaired O2 unloading from stored blood results in diffusion-limited O2 release at tissues: evidence from human kidneys. Blood 2023; blood.2023022385. doi: https://doi.org/10.1182/blood.2023022385
9. Edwards A, Kurtcuoglu V. Renal blood flow and oxygenation. Pflugers Arch. 2022 Aug;474(8):759-770.
10. Evans RG, Gardiner BS, Smith DW, O'Connor PM. Intrarenal oxy-genation: unique challenges and the biophysical basis of homeostasis. Am J Physiol Renal Physiol (2008) 295: F1259–F1270.
11. Evans, R.G. Oxygen regulation in biological systems. Am J Physiol Regul Integr Comp Physiol (2016) 310: R673 - R678.
12. Evans RG, Lankadeva YR, Cochrane AD, Marino B, Iguchi N, Zhu MZL, Hood SG, Smith JA, Bellomo R, Gardiner BS, Lee CJ, Smith DW, May CN, Evans RG, et al. Renal haemodynamics and oxygenation during and after cardiac surgery and cardiopulmonary bypass. Acta Physiol (Oxf). 2018;222(3). Epub 2017 Nov 30. PMID: 29127739. https://doi.org/10.1111/apha.12995.
13. Fox, Lawrence S., et al. "Relationship of whole body oxygen consumption to perfusion flow rate during hypothermic cardiopulmonary bypass." The Journal of Thoracic and Cardiovascular Surgery 83.2 (1982): 239-248.
14. Friedman, Gilberto, et al. "Oxygen supply dependency can characterize septic shock." Intensive care medicine 24 (1998): 118-123.
15. Guzy, R.D. and Schumacker, P.T. Oxygen sensing by mitochondria at complex III: the paradox of increased reactive oxygen species during hypoxia. Experimental Physiology (2006) 91: 807-819.

medRxiv preprint doi: https://doi.org/10.1101/2024.03.18.24304520; this version posted March 19, 2024. The copyright holder for this preprint (which was not certified by peer review) is the author/funder, who has granted medRxiv a license to display the preprint in perpetuity. It is made available under a CC-BY-NC-ND 4.0 International license .

16. Hayward, A., et al. "Oxygen Delivery in Pediatric Cardiac Surgery and its Prediction of Acute Kidney Injury using Machine Learning." Journal of Thoracic and Cardiovascular Surgery. (2023);165(4):1505-1516.
17. Hendrix, Rik HJ, Yuri M. Ganushchak, and Patrick W. Weerwind. "Oxygen delivery, oxygen consumption and decreased kidney function after cardiopulmonary bypass." PLoS One 14.11 (2019): e0225541.
18. Jakutis G, Norkienė I, Ringaitienė D, Jovaiša T. Severity of hyperoxia as a risk factor in patients undergoing on-pump cardiac surgery. Acta Med Litu. 2017;24(3):153-158.
19. Kirklin, James K., and Eugene H. Blackstone. Kirklin/Barratt-Boyes Cardiac Surgery: Expert Consult-Online and Print (2-Volume Set). Vol. 1. Elsevier Health Sciences, 2012.
20. Khwaja, Arif. "KDIGO clinical practice guidelines for acute kidney injury." Nephron Clinical Practice 120.4 (2012): c179-c184.
21. Lane N.Oxygen: The Molecule that Made the World. Oxford: Oxford University, 2003.
22. Lenzen S. A fresh view of glycolysis and glucokinase regulation: history and current status. J Biol Chem. 2014 May 02;289(18):12189-94
23. Lubarsky, David A., et al. "Defining the relationship of oxygen delivery and consumption: use of biologic system models." Journal of Surgical Research 58.5 (1995): 503-508.
24. Mahani, Alireza S., and Mansour T. A. Sharabiani (2017). "Multivariate-From-Univariate MCMC Sampler: The R Package MfUSampler." Journal of Statistical Software, Code Snippets, 78(1), 1-22. doi:10.18637/jss.v078.c01.
25. Naik SK, Elliott MJ. Ultrafiltration and paediatric cardiopulmonary bypass. Perfusion. 1993;8:101-12.
26. Paneth, Matthias, et al. "Physiologic studies upon prolonged cardiopulmonary by-pass with the pump-oxygenator with particular reference to (1) acid-base balance,(2) siphon caval drainage." Journal of Thoracic Surgery 34.5 (1957): 570-579.

medRxiv preprint doi: https://doi.org/10.1101/2024.03.18.24304520; this version posted March 19, 2024. The copyright holder for this preprint (which was not certified by peer review) is the author/funder, who has granted medRxiv a license to display the preprint in perpetuity. It is made available under a CC-BY-NC-ND 4.0 International license .

27. R Core Team (2021). “R: A language and environment for statistical computing.” R Foundation for Statistical Computing, Vienna, Austria. URL https://www.R-project.org/.
28. Ranucci, Marco, et al. "Goal-directed perfusion to reduce acute kidney injury: a randomized trial." The Journal of thoracic and cardiovascular surgery 156.5 (2018): 1918-1927.
29. Resseguie, E.A., Staversky, R.J., Brookes, P.S., and O’Reilly, M.A. Hyperoxia activates ATM independent from mitochondrial ROS and dysfunction. Redox Biology, 2015 (5): 176-185.
30. L. Rogers, K. L. Brown, R. C. Franklin, G. Ambler, D. Anderson, D. J. Barron, et al. Improving Risk Adjustment for Mortality After Pediatric Cardiac Surgery: The UK PRAiS2 Model. The Annals of Thoracic Surgery 2017 Vol. 104 Issue 1 Pages 211-219.
31. Smith HW, Chasis H, Goldring W, Ranges HA. Glomerular dynamics in the normal human kidney. J Clin Invest. 1940;19:751–764. doi: 10.1172/JCI101180.
32. Starr, Albert. "Oxygen consumption during cardiopulmonary bypass." The Journal of Thoracic and Cardiovascular Surgery 38.1 (1959): 46-56.
33. Wilson, D.F., Harrison, D.K., and Vinogradov, S.A. Oxygen, pH, and mitochondrial oxidative phosphorylation J Appl Physiol (2012) 113: 1838–1845.
34. Wolff, Christopher. Oxygen Delivery: The Principal Role of the Circulation. Advances in experimental medicine and biology. (2013). 789. 37-42.
35. Yi Q, Li K, Jian Z, et al. Risk factors for acute kidney injury after cardiovascular surgery: evidence from 2157 cases and 49 777 controls: a meta-analysis. Cardiorenal Med. 2016;6:237–50.
36. Yoshida, T., Prudent, M. & D'Alessandro, A. Red blood cell storage lesion: causes
and potential clinical consequences. Blood Transfus 17, 27-52 (2019).
37. Young RW. Hyperoxia: a review of the risks and benefits in adult cardiac surgery. J Extra Corpor Technol. 2012 Dec;44(4):241-9.

medRxiv preprint doi: https://doi.org/10.1101/2024.03.18.24304520; this version posted March 19, 2024. The copyright holder for this preprint (which was not certified by peer review) is the author/funder, who has granted medRxiv a license to display the preprint in perpetuity. It is made available under a CC-BY-NC-ND 4.0 International license .

Tables

Table 1

Variable	Value
Number of operations/patients	754/691
Age at operation (months) Range	7.6 [3.0-46.7] 0.12-218.8
Age group (at operation) Neonates (0-30 days) Infants (1-12 months) Children (1-18 years)	 321 (43) 319 (42) 114 (15)
Sex Male Female	 384 (56) 307 (44)
Ethnicity White BAME <Not Available>	 344 (50) 257 (37) 90 (13)
Antenatal diagnosis Yes No <Not Available>	 285 (38) 428 (57) 41 (5)
30-day mortality Expected (using PRAiS) Observed	 12 (1.6) 4 (0.5)
KIDGO score 0 1 2 3	 293 (39) 256 (34) 122 (16) 83 (11)

Table 1: Summary of patients and their outcomes. Numbers in brackets represent interquartile ranges for numeric variables, while numbers in parentheses represent percentages for discrete variables. Note that for sex and ethnicity, the counts and percentages are reported at the patient level, while for other variables (including age), the figures are reported at the operation level. BAME: Black, Asian and Minority Ethnic.

medRxiv preprint doi: https://doi.org/10.1101/2024.03.18.24304520; this version posted March 19, 2024. The copyright holder for this preprint (which was not certified by peer review) is the author/funder, who has granted medRxiv a license to display the preprint in perpetuity. It is made available under a CC-BY-NC-ND 4.0 International license .

Table 2

	GARIX+(7)		Kirklin
Parameter	**estimate**	**95% CI**	**estimate**
R-squared	75.5%	58.8% - 92.1%	65%
a	39.5	24.9 - 60.0	35
b	0.94	0.26 - 1.78	0.42

Table 2: Comparison of R-squared and fit parameters from GARIX+(7) simulations mimicking Kirklin experiments, against the Kirklin fit, reported in Fox et al (1982). See Supp Mat B for definitions of ‘a’ and ‘b’.

Table 3

		tDO_2i (mL/min/m^2)	
Temperature (C)	**tVO_2i (mL/min/m^2)**	**OER_{max} = 50%**	**OER_{max} = 20%**
15	16	32	78
20	23	46	115
25	34	78	171
30	51	102	252
37	87	174	436

Table 2: Target (indexed) oxygen consumption (tVO_2i) and threshold (indexed) oxygen delivery (tDO_2i) - assuming a maximum OER of 50% and 20% - at different temperatures, as predicted by the GARIX+(7) model of Equation 9, fitted to our granular perfusion data.

medRxiv preprint doi: https://doi.org/10.1101/2024.03.18.24304520; this version posted March 19, 2024. The copyright holder for this preprint (which was not certified by peer review) is the author/funder, who has granted medRxiv a license to display the preprint in perpetuity. It is made available under a CC-BY-NC-ND 4.0 International license .

Figures

Figure 1

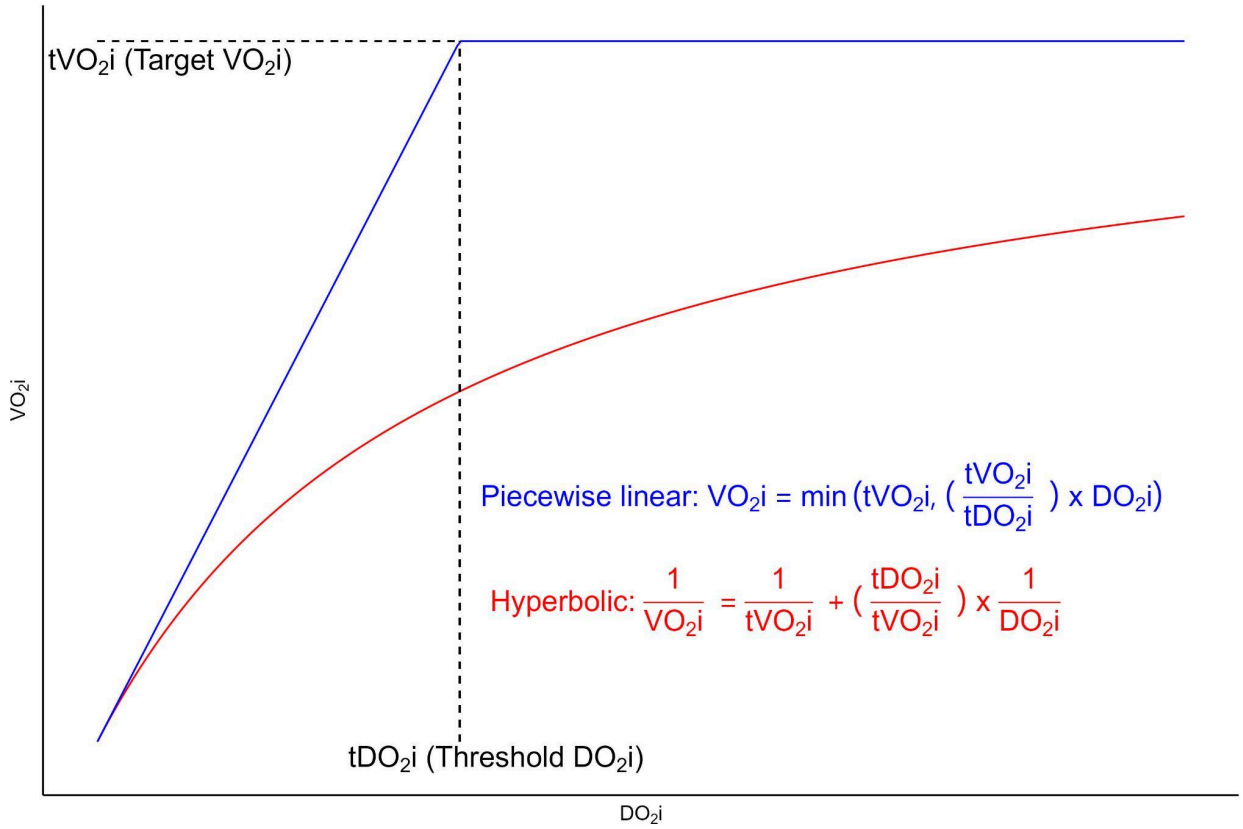

Figure 1: Schematic of a piecewise-linear (blue) model, and its corresponding hyperbolic (red) model of indexed oxygen consumption (VO_2i) vs. indexed oxygen delivery (DO_2i). The two equations describe models that both go through origin (DO_2i = 0, VO_2i = 0), have the same slope at origin (i.e., tVO_2i/tDO_2i), and the same maximum value for VO_2i (i.e., tVO_2i). As such, this hyperbolic equation can be considered the 'smooth' counterpart to the piecewise-linear equation.

medRxiv preprint doi: https://doi.org/10.1101/2024.03.18.24304520; this version posted March 19, 2024. The copyright holder for this preprint (which was not certified by peer review) is the author/funder, who has granted medRxiv a license to display the preprint in perpetuity. It is made available under a CC-BY-NC-ND 4.0 International license .

Figure 2

What does GARIX+ stand for?

- GARIX: Global AutoRegressive Integrated time-series model with EXogenous variables
- GARIX+: GARIX, augmented with a 'disequilibrium' force

What is the aim of GARIX+? Predicting near-term changes in OER during CPB as a function of *system history*, *present state*, and *intended actions* (perspective #1):

- *System history*: Past changes in CI, Hb, SaO_2, temperature and OER
- *Present state*: Current values of CI, Hb, SaO_2, temperature and OER
- *Intended actions*: Planned changes in CI, Hb, SaO_2 and temperature.

Alternative interpretation - GARIX+ model describes OER changes as a function of *autoregressive*, *disequilibrium*, and *exogenous* forces (perspective #2):

- *Disequilibrium* force seeks to change oxygen consumption (VO_2i) - via changing OER - to bring it in line with oxygen demand (tVO_2i), as dictated by temperature.
- *Autoregressive* force serves to reverse random fluctuations in OER, thus creating further stability when system is near equilibrium.
- *Exogenous* force reflects short-term impact of changes in CI, Hb, SaO_2 and temperature on OER so as to keep VO_2i in line with tVO_2i.

The GARIX+ model maps each of the three forces above to a collection of regression terms, referred to as term groups (TGs) in the text.

Model scope and idealisations (current version):

- Model is global, i.e. parameters are shared across all patients (homogeneity assumption).
- Focus is on haemoglobin-bound oxygen (excluding dissolved oxygen).
- CI, Hb and SaO_2 are considered exogenous, i.e., fully controllable by the perfusionist.
- System noise is homoscedastic, i.e., random fluctuations in OER have the same overall strength at all times and across all patients.
- Dependence of tVO_2i on temperature follows the Van't Hoff (Q10) specification.

Figure 2: Conceptual summary of the GARIX+ model, proposed in this paper.

medRxiv preprint doi: https://doi.org/10.1101/2024.03.18.24304520; this version posted March 19, 2024. The copyright holder for this preprint (which was not certified by peer review) is the author/funder, who has granted medRxiv a license to display the preprint in perpetuity. It is made available under a CC-BY-NC-ND 4.0 International license .

Figure 3

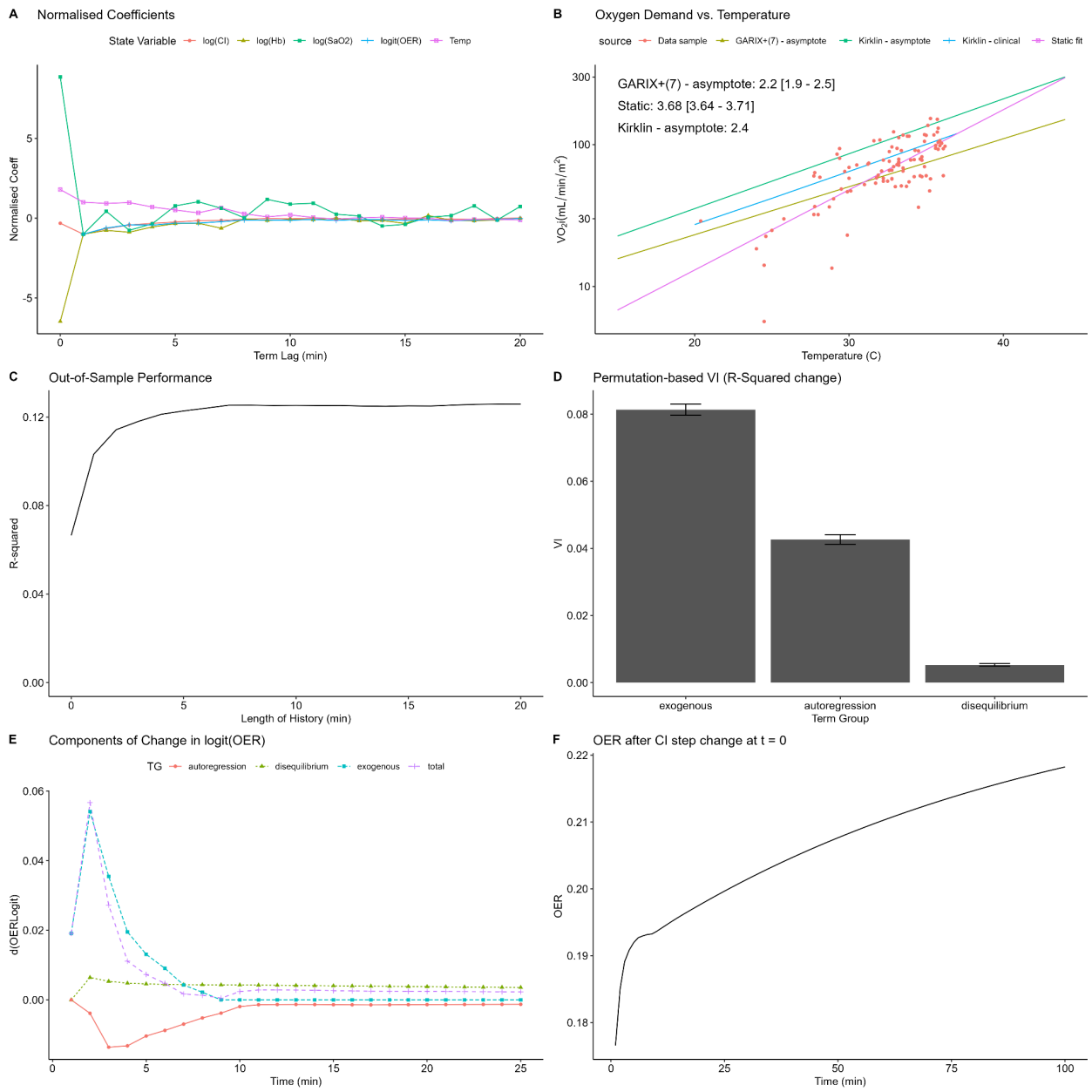

Figure 3: Results for fitting GARIX+ models of Equation 9 to the CPB perfusion data. **A**: Coefficients for each state variable are divided by their value at lag = 1 minute. Coefficients of $logit(OER)$ (the endogenous variable) stop at lag = 1 (change from one minute ago to now), while exogenous variables continue to lag = 0 (change from now to one minute from now). **B**: Comparison of models for Oxygen demand ($tVO2i$) vs. body temperature (note the logarithmic scale of the y axis). The 'Kirklin - asymptote' line

medRxiv preprint doi: https://doi.org/10.1101/2024.03.18.24304520; this version posted March 19, 2024. The copyright holder for this preprint (which was not certified by peer review) is the author/funder, who has granted medRxiv a license to display the preprint in perpetuity. It is made available under a CC-BY-NC-ND 4.0 International license .

(green) is from Kirklin and Blackstone (2012), Equation 2A-3, with CI set to infinity, i.e., asymptotic value of the hyperbolic curve (see Kirklin Equation). The 'Kirklin - clinical' line (blue) is taken from Figure 2-11 of the same textbook, using the small X's in the figure, which are referred to as oxygen consumption levels corresponding to clinical flow rates used at temperatures 20°C (27 mL/min/m^2), 25°C (42 mL/min/m^2), 30°C (65 mL/min/m^2) and 37°C (120 mL/min/m^2). Mustard-colour points are 100 random samples of the training data. Purple line represents the Static Model, and the red line corresponds to the asymptotic value (tVO_2i) of the GARIX+(7) model. Printed numbers indicate the Q10 values derived using various methods, with brackets showing 95% confidence interval for each Q10 value (no confidence interval available for Kirklin). **C**: Out-of-sample R-squared (using average of 10-times repeated, 5-fold cross-validated model predictions) vs. length of history (parameter N) used in the GARIX+(N) model. **D**: PVI by TG, using 5-fold cross-validation, and 10 random shufflings of target TGs within each prediction fold. Error bars are based on standard deviations of the decline in out-of-sample R-squared across the random shufflings. **E**: Decomposition of predicted changes in $logit(OER)$ in response to a 25% decrease in cardiac index at t = 0 ($\log(CI)$, becoming 0.714). The system is assumed to be in equilibrium at t = 0, with state variables being $\log(CI) = 1.00$, $\log(Hb) = 2.31$, $\log(SaO_2) = 4.60$, $T = 33.1C$. Simulations were run in deterministic mode. **F**: OER vs time since change in CI, corresponding to the same experiment as in Panel E. The y values are inverse-logit transformed from the cumulative sum of the 'total' time series in Panel E.

medRxiv preprint doi: https://doi.org/10.1101/2024.03.18.24304520; this version posted March 19, 2024. The copyright holder for this preprint (which was not certified by peer review) is the author/funder, who has granted medRxiv a license to display the preprint in perpetuity. It is made available under a CC-BY-NC-ND 4.0 International license .

Figure 4

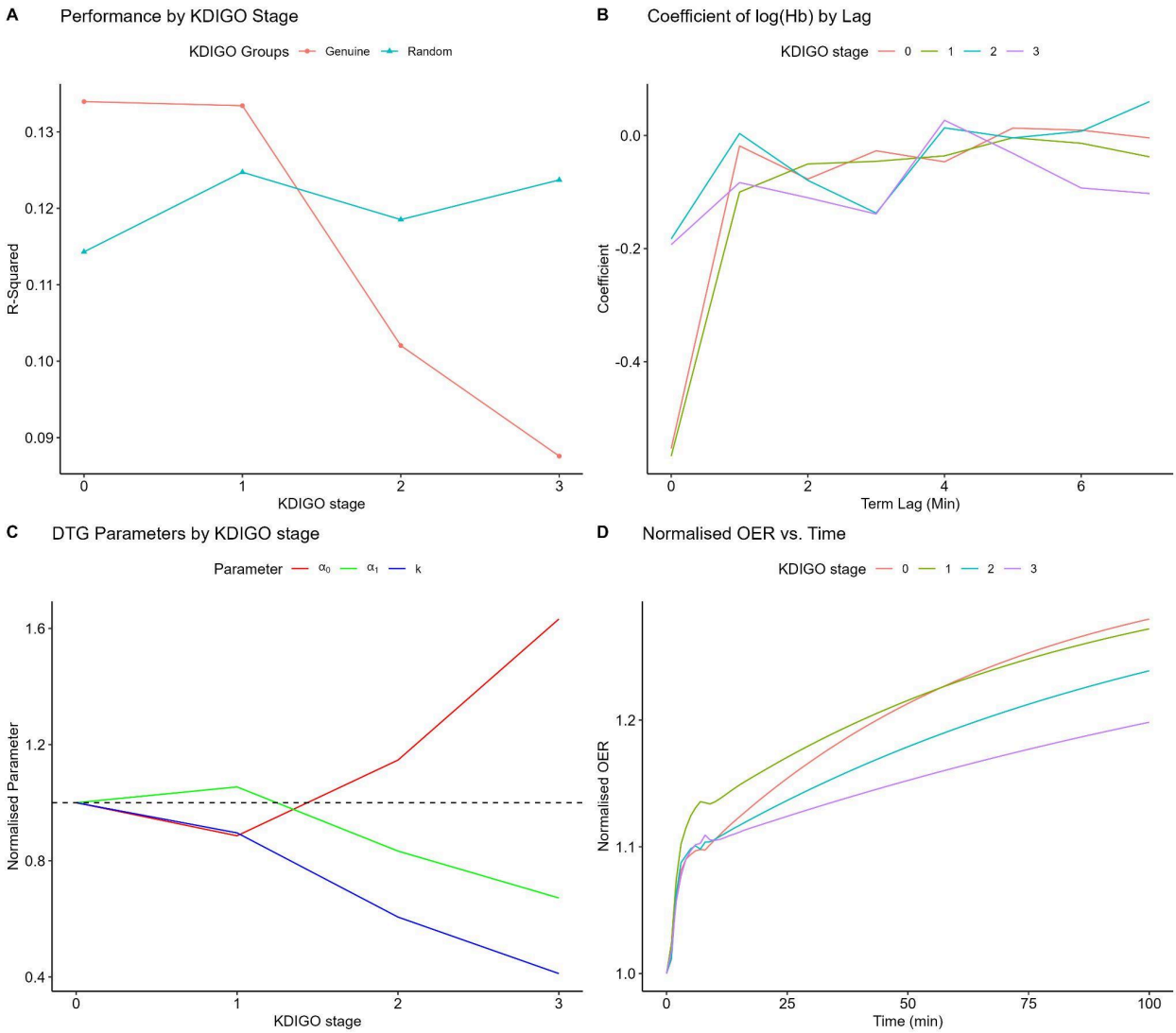

Figure 4: Subgroup analysis of the GARIX+(7) model by AKI severity. **A**: Out-of-sample R-squared (using average of 10-times repeated, 5-fold cross-validated predictions) vs. KDIGO stage of patients selected for training the models (red line), labelled as 'Genuine'. The blue line, labelled as 'Random', corresponds to out-of-sample R-squared (using identical CV settings) over 10 random splits of the entire data into datasets of the same size as those corresponding to each KDIGO stage. **B**: Coefficient of exogenous terms involving 'Hb' (haemoglobin), as a function of lag (in minutes), split by KIDIGO stage of patients used in the training data. **C**: Parameters of the DTG - each normalised

medRxiv preprint doi: https://doi.org/10.1101/2024.03.18.24304520; this version posted March 19, 2024. The copyright holder for this preprint (which was not certified by peer review) is the author/funder, who has granted medRxiv a license to display the preprint in perpetuity. It is made available under a CC-BY-NC-ND 4.0 International license .

by its value at KDIGO = 0 - as a function of the KDIGO stage of patients included in training the data. α_0 and α_1 correspond to the Van't Hoff model that predicts the logarithm of tVO2i as a function of body temperature. **D**: OER - normalised by its value at t = 0 (the time at which cardiac index is decreased by 25%) using deterministic simulation by models trained exclusively on patients with different levels of KDIGO stage; initial (equilibrium) conditions by KIDIGO stage (0/1/2/3): log(ci) = 1.02/0.993/0.977/1.02, log(Hb) = 2.30/2.30/2.31/2.33, log(SaO2) = 4.6 (all groups), temp = 33.4/33.1/32.9/33.2, logit(OER) = -1.48/-1.50/-1.77/-1.48.

medRxiv preprint doi: https://doi.org/10.1101/2024.03.18.24304520; this version posted March 19, 2024. The copyright holder for this preprint (which was not certified by peer review) is the author/funder, who has granted medRxiv a license to display the preprint in perpetuity. It is made available under a CC-BY-NC-ND 4.0 International license .

Figure 5

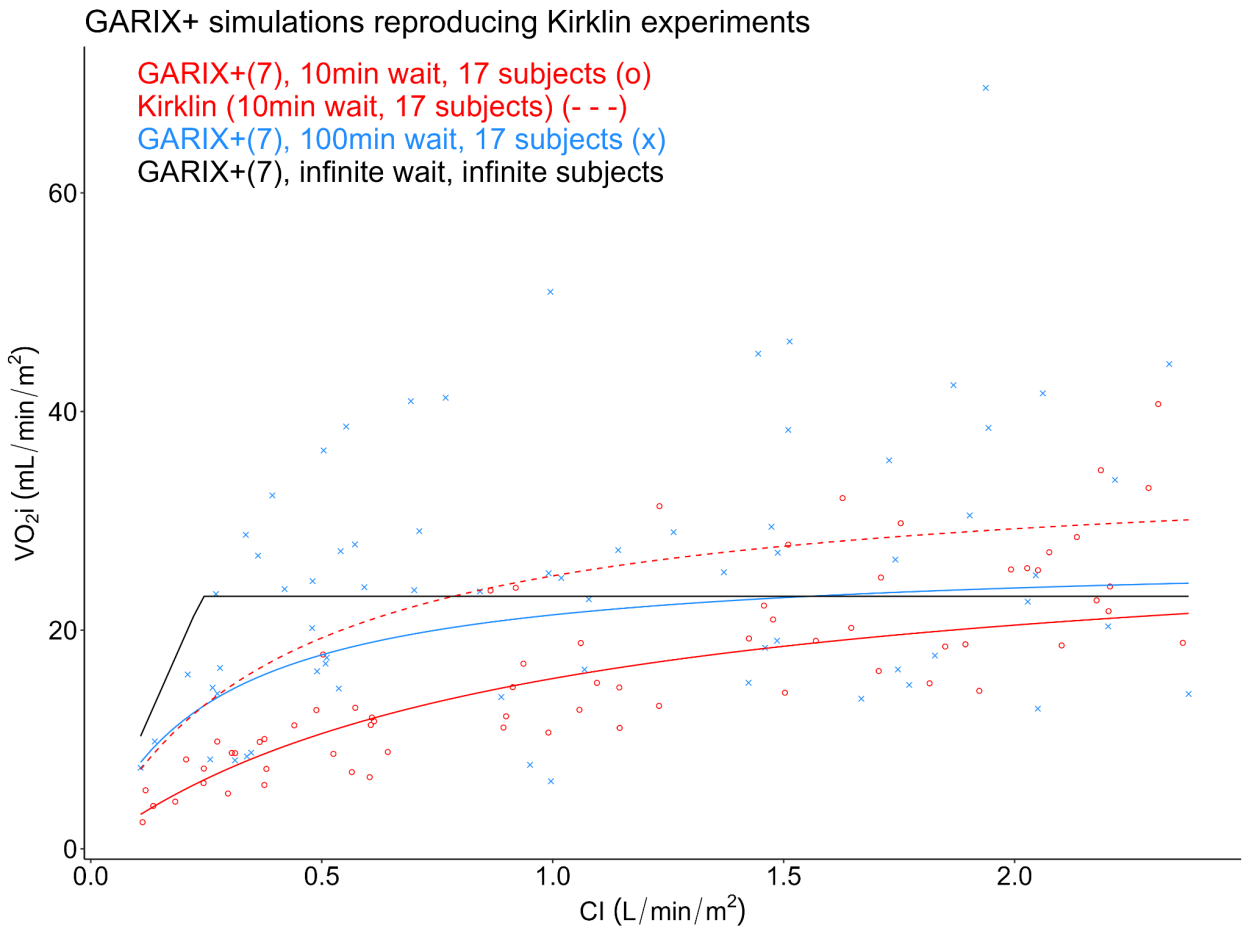

Figure 5: Comparison of VO_2i vs. CI curves, produced by the GARIX+(7) model (simulation-based) and Kirklin's hyperbolic model (human experiments; Fox et al, 1982). Red o's show results of a sample simulation using GARIX+(7), with settings that closely match the Fox et al experiments (see Supp Mat B), including a 10-minute wait after each change to the CI. Red curve of the same colour is the hyperbolic fit to that data. Blue x's are GARIX+(7) simulations with the same settings, except wait times are increased from 10 minutes to 100 minutes. The blue curve, again, shows the hyperbolic fit to that data. The black, piecewise linear line shows the results for infinite wait time and averaging over an infinite pool of (simulation) subjects. Dotted red curve is the hyperbolic model of Kirklin, based on experiments of Fox et al (1982).

medRxiv preprint doi: https://doi.org/10.1101/2024.03.18.24304520; this version posted March 19, 2024. The copyright holder for this preprint (which was not certified by peer review) is the author/funder, who has granted medRxiv a license to display the preprint in perpetuity. It is made available under a CC-BY-NC-ND 4.0 International license .

Figure 6

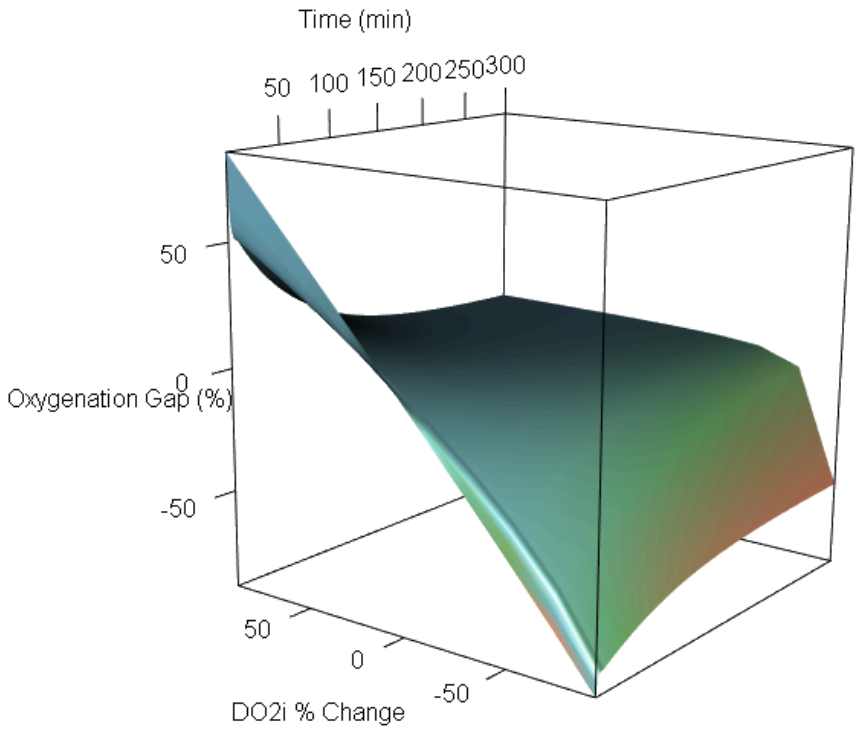

Figure 6: Oxygenation gap (OG) as a function of % change in DO2i (via a change in CI), at different wait times, using deterministic simulation with a GARIX+(7) model. State variables are log(ci) = 0.217, log(Hb) = 1.96, log(SaO2) = 4.6, temp = 20, logit(OER) = -1.42. Positive OGs indicate over-oxygenation and negative OGs reflect under-oxygenation. See text for exact definitions.

medRxiv preprint doi: https://doi.org/10.1101/2024.03.18.24304520; this version posted March 19, 2024. The copyright holder for this preprint (which was not certified by peer review) is the author/funder, who has granted medRxiv a license to display the preprint in perpetuity. It is made available under a CC-BY-NC-ND 4.0 International license .

Figure 7

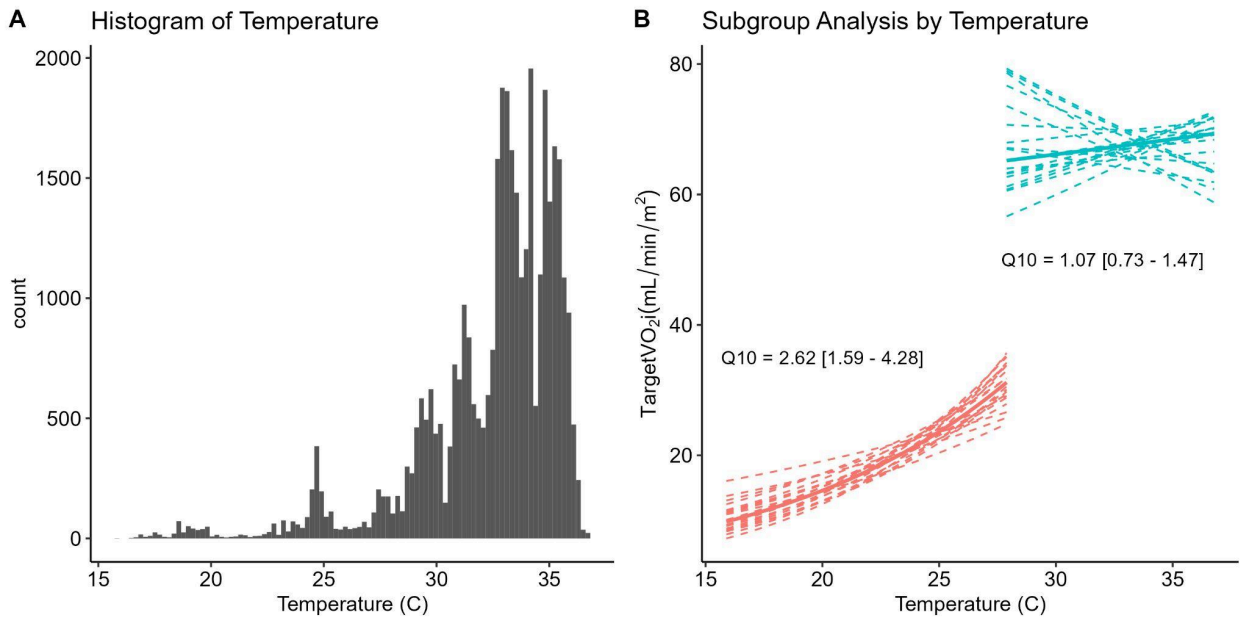

Figure 7: Subgroup analysis of Q10 by temperature range, using the GARIX+(7) model. **A**: Histogram of temperature readings in perfusion data, reflecting high concentration of data in the >30C range, with a smaller peak near 25C. **B**: Predicted tVO2i as a function of temperature, in low-temp range (15-28 C) (red) and high-temp range (28-38 C) (blue); dotted lines are based on 10 random samples from the estimated joint distribution of parameters, and solid lines are based on median values.

medRxiv preprint doi: https://doi.org/10.1101/2024.03.18.24304520; this version posted March 19, 2024. The copyright holder for this preprint (which was not certified by peer review) is the author/funder, who has granted medRxiv a license to display the preprint in perpetuity. It is made available under a CC-BY-NC-ND 4.0 International license .

Supplementary Material

A: Approximate Equivalence of Van't Hoff and Arrhenius Specifications

The Arrhenius and Van't Hoff formulations are the best known parametric forms used to describe the relationship between temperature and oxygen consumption. It can be demonstrated that, as long as temperature changes are small compared to their absolute values, *when expressed in Kelvins*, the two specifications are approximately equivalent. In this manuscript, the Van't Hoff specification has been adopted, which is consistent with the widely recognised concept of Q10, the multiplicative increase in RMR for every 10 degrees C increase in body temperature.

The Arrhenius equation, after mapping the concept of chemical reaction rate to metabolism and hence oxygen consumption, would require the logarithm of oxygen consumption to be a linear function of the inverse of temperature, expressed in Kelvins (T_k):

$$log(VO_2i) = a + b/T_k \quad \text{(A.1)}$$

Let's express T_K in terms of its deviations (ΔT) from a baseline value, T_0:

$$T_K = T_0 + \Delta T. \quad \text{(A.2)}$$

Equation (A.1) can be rewritten as:

$$log(VO_2i) = a + b/(T_0 + \Delta T) \quad \text{(A.3)}$$

If $\Delta T << T_0$, i.e., if changes in temperature are small compared to its baseline value, in Kelvins, then a first-order, Taylor-series expansion is used to rewrite Equation (A.3):

$$log(VO_2i) = a + b/(T_0(1 + \Delta T/T_0)) \approx a + (b/T_0)(1 - \Delta T/T_0) = (a + b/T_0) + (- b/T_0^2)\,\Delta T$$

Note that the last expression on the right is a linear function of temperature change, ΔT. This is simply the Van't Hoff specification, i.e., logarithm of VO_2i being a linear function of temperature. (Keep in mind that one Kelvin change equals one Celsius change in temperature, i.e., ΔT would be identical whether expressed in Kelvins or Celsius.)

medRxiv preprint doi: https://doi.org/10.1101/2024.03.18.24304520; this version posted March 19, 2024. The copyright holder for this preprint (which was not certified by peer review) is the author/funder, who has granted medRxiv a license to display the preprint in perpetuity. It is made available under a CC-BY-NC-ND 4.0 International license .

B: Experimental Setup and Model Specification of Fox et al (1982)

Table 1 in Fox et al (1982) was consulted for constructing the random sequence of CI values for each simulated subject who received 4 step-function changes to their CI during the simulations. (The initial value of CI was 2.2 L/min/m^2 for all subjects.) This means that, for each step-function change in CI, one of the four possible CI bands listed in Table 1 is first randomly selected and then a random number is drawn from the normal distribution associated with that CI band, according to the mean and standard deviation values listed therein. Fox *et al.*, fitted a hyperbolic model to their experimental data, which assumes 1/VO_2i to be a linear function of 1/CI: $VO_2i = a \times CI / (b + CI)$, with $a = 35$, $b = 0.42$. Note that this equation is equivalent to Equation 6 for $T = 20C$.

C: GARIX+ Model Diagnostics

Panel A of Figure C-1 shows the combined autocorrelation function (ACF) plot of GARIX+(7) model residuals across all segments. For comparison, Panel B shows the same plot, where model residuals are replaced with white noise. The overall similarity of plots - with the average (red) line being close to the y = 0 line - indicates that model residuals are well-behaved. Panel C shows the ACF plot for the absolute of model residuals, and Panel D shows the ACF of the absolute of white noise. The discrepancy between these two panels is a sign that there is information in the magnitude of residual noise, i.e., heteroscedasticity. Incorporating heteroscedasticity into the GARIX+ model is a topic of future research.

medRxiv preprint doi: https://doi.org/10.1101/2024.03.18.24304520; this version posted March 19, 2024. The copyright holder for this preprint (which was not certified by peer review) is the author/funder, who has granted medRxiv a license to display the preprint in perpetuity. It is made available under a CC-BY-NC-ND 4.0 International license .

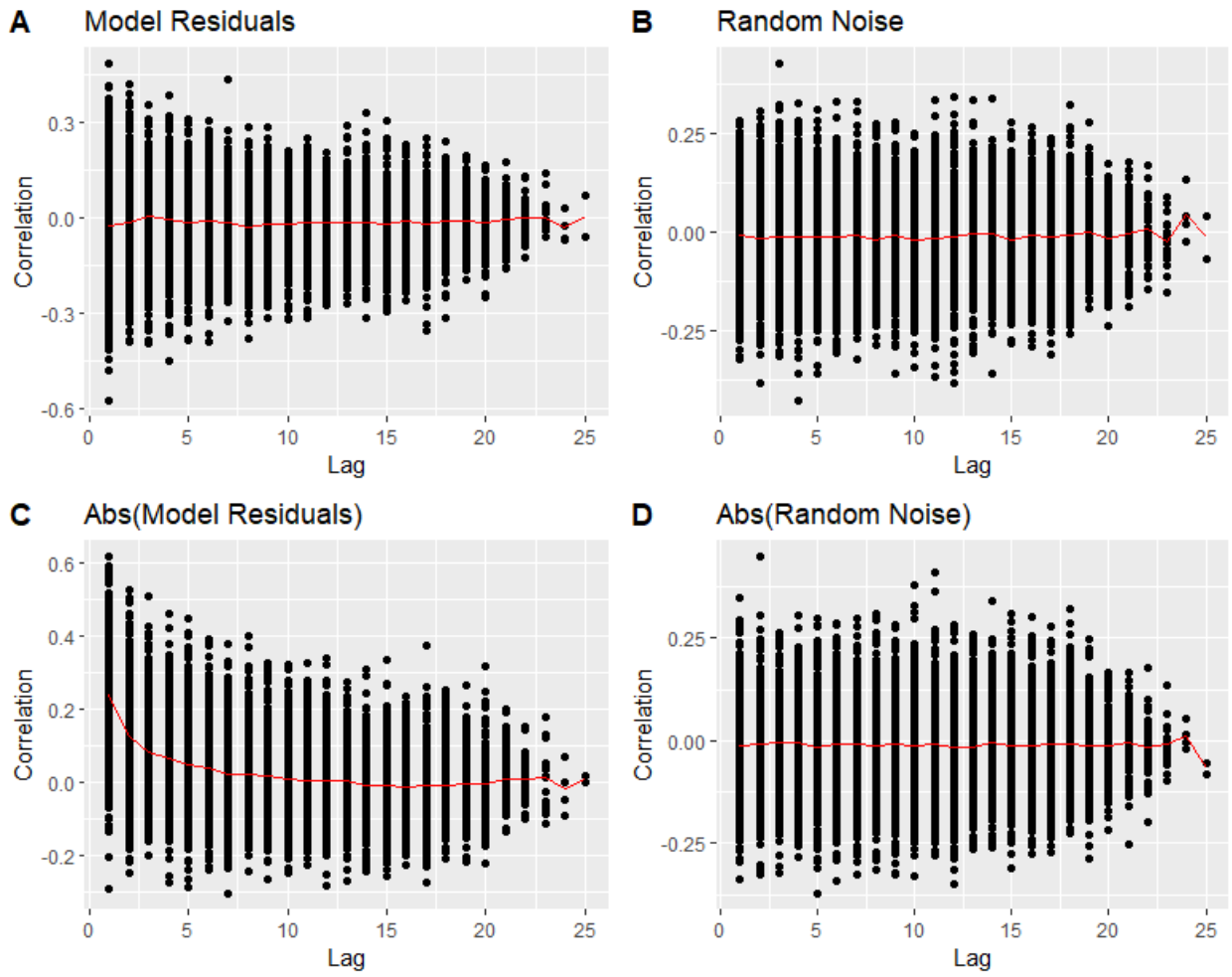

Figure C-1: Combined autocorrelation plots (across all data segments) for GARIX+(7) model residuals (Panel A), i.i.d. Gaussian noise (Panel B), absolute of model residuals (Panel C), and absolute of i.i.d. Gaussian noise (Panel D). Red lines in each panel show average correlation at each lag across all contributing segments. A minimum segment length of 50 minutes was imposed on the data.

D: Statistical Significance of GARIX+ Coefficients

The supplementary file, GARIX_20_model_coefficients_supp_mat.csv, shows the list of coefficients and their statistical significance for the GARIX+(20) model. The majority of terms have statistical significance for up to 5-10 minutes of lag, and the terms corresponding to recent history have particularly high significance. An exception is SaO_2, which is only highly significant at lag = 0 (corresponding to change from t to t+1).